A contribution of methods for analysis of laminated composites and adhesive joints

Lauridsen, Peter Riddersholm

DOI (link to publication from Publisher):
10.54337/aau448597214

Publication date:
2021

Document Version
Publisher's PDF, also known as Version of record

A CONTRIBUTION OF METHODS FOR ANALYSIS OF LAMINATED COMPOSITES AND ADHESIVE JOINTS

BY
PETER RIDDERSHOLM LAURIDSEN

DISSERTATION SUBMITTED 2021

AALBORG UNIVERSITY
DENMARK

A contribution of methods for analysis of laminated composites and adhesive joints

PhD Dissertation

Peter Riddersholm Lauridsen

Aalborg University
Department of the Built Environment
Niels Bohrs Vej 8
DK-6700 Esbjerg

Dissertation submitted: April, 2021

PhD supervisor: Associate Professor, Anders Schmidt Kristensen
Aalborg University Esbjerg,
Department of Energy Technology

PhD committee: Associate Professor Peter Frigaard (Chairman)
Aalborg University

Dr.-Ing. Claudio Balzani
Leibniz University Hannover

Associate Professor Jan Høgsberg
Technical University of Denmark

PhD Series: Faculty of Engineering and Science, Aalborg University

Department: Department of the Build Environment

ISSN (online): 2446-1636
ISBN (online): 978-87-7210-936-7

Published by:
Aalborg University Press
Kroghstræde 3
DK – 9220 Aalborg Ø
Phone: +45 99407140
aauf@forlag.aau.dk
forlag.aau.dk

Printed in Denmark by Rosendahls, 2021

Abstract

Laminated composites and adhesive joints are extensively used in structures such as wind turbine blades, and the performance of these are pushed to the failure limits in order to obtain stiffer, stronger and lighter blades. To achieve this is fracture resistance, fatigue strength and crack growth rate are some of the most important parameters to identify. This means, that new approaches are required, and with basis in this the presented PhD project will contribute with some novel methods. These new methods will expand the possibilities in testing and designing modern wind turbine blades, and still ensure structural integrity.

First contribution is an unseen test fixture and method (TP-MMB), which is used for determination of mode mixity fracture resistance in laminated composites and adhesive joints. The developed test fixture is designed for coupon testing and fits into a standard tensile testing machine. Moreover, it requires a minimum of measuring equipment for this test method, and validation of this method as well as apparatus have shown fine results in a quasi-static test. This can be concluded, as these results are in good accordance to well known theory and principles.

Second part is a contribution of three Finite Element based approaches for determination of so called Brazier forces or contributing forces, which is a second order effect also referred to as geometric non-linearity. The two first algorithms are special designed for respectively bending or torsion in uniform cross sections, and the last algorithm is able to handle all types of geometries and load cases. All presented approaches bring down the computational effort, and accuracy of the computed stress field is still relatively high. The reduction of computational savings will dependent on the degree of non-linearity and size of Finite Element model. Furthermore, the geometric non-linearity is especially critical in slender composite structures like wind turbine blades, as these effects can have a significant impact on the stress field and thereby on fatigue life in wind turbine blades. This method would therefore often be to prefer in fatigue analysis of wind turbine blades.

The aforementioned contributions are designed for analysis of laminated composites and adhesive joints. It can be concluded that both contributions are suitable for the wind turbine industry, as these contributions perform well and has a degree of novelty in this field of research.

Resume

Laminater og limsamlinger er i vid udstrækning anvendt i konstruktioner såsom vindmøllevinger, og ydeevnen af disse skubbes til svigtgrænserne for at opnå stivere, stærkere og lettere vinger. For at opnå dette er brudsejhed, udmattelsesstyrke og revnevækst pr. cyklus nogle af de vigtigste parametre at identificere, og det betyder at nye metoder er påkrævet. Med udgangspunkt i dette vil det præsenterede PhD projekt bidrage med nogle nye metoder. Disse nye metoder vil udvide mulighederne for at teste og designe moderne vindvindmøllevinger og stadig sikre strukturel integritet.

Første bidrag er et uset testfikstur og metode (TP-MMB), der anvendes til bestemmelse af brudsejhed i laminater og limsamlinger. Det udviklede testfikstur er designet til relativt små testemner og passer ind i en standard trækprøvningsmaskine, og desuden så kræves et minimum af måleudstyr til denne metode. Validering af metode såvel som fikstur har vist gode resultater i en kvasistatisk test. Dette kan konkluderes da resultaterne er i god overensstemmelse med velkendt teori og principper.

Anden del er tre Finite Element baserede bidrag til bestemmelse af såkaldte Brazierkræfter eller bidragende kræfter. Dette er en andenordenseffekt som også kan refereres til som geometrisk ikke-linearitet. De to første algoritmer er specielt designet til henholdsvis bøjning eller vridning i ensartede tværsnit, og den sidste algoritme er i stand til at håndtere alle typer geometrier og belastningstilfælde. De præsenterede metoder nedbringer den computermæssige beregningstid, og nøjagtigheden af de beregnede spændinger er stadig relativ høj. Reduktionen af beregningstiden afhænger af graden af ikke-linearitet og størrelsen af Finite Element modellen. Udover det er geometrisk ikke-linearitet især kritisk i slanke kompositkonstruktioner som fx vindmøllevinger, da disse effekter kan have en betydelig indflydelse på spændingerne og derved påvirke udmattelseslevetiden i vindmøllevingerne. Denne metode vil ofte derfor være at foretrække i en udmattelsesanalyse af vindmøllevinger, da nøjagtigheden er høj, og tidsforbruget er relativt lavt.

Ovennævnte bidrag er designet til analyse af laminater og limsamlinger, og det kan konkluderes, at begge bidrag er egnede til vindmølleindustrien, da disse bidrag yder en relativ høj præcision og indeholder en grad af nyhedsværdi i dette forskningsfelt.

Contents

Thesis Details

Thesis Title:	A contribution of methods for analysis of laminated composites and adhesive joints
PhD Student:	MSc Mechanical Design, Peter Riddersholm Lauridsen Aalborg University Esbjerg
Supervisor:	Assoc. Prof., Head of Campus, Anders Schmidt Kristensen Aalborg University Esbjerg, Department of Energy Technology

The main body of this thesis consists of the following papers.

[A] Peter Riddersholm Lauridsen and Anders Schmidt Kristensen, "A Two Point Mixed Mode Bending (TP-MMB) test method for determination of fracture resistance in adhesive joints and laminated composites," *Accepted with minor revisions, Journal of Composite Materials, SAGE Journals*, ISSN: 0021-9983, 2020.

[B] Peter Riddersholm Lauridsen and Anders Schmidt Kristensen, "A linear approach to non-linear geometric effects in slender composite structures," *Submitted to Wind Engineering, SAGE Journals*, ISSN: 0309-524X, 2020.

[C] Peter Riddersholm Lauridsen, Jan Anike Nikolajsen and Lars Damkilde, "Implementation of the generalized Brazier effect in linear analysis of wind turbine blades," *Conference, Proceedings of the 29th Nordic Seminar on Computational Mechanics (NSCM-29), Chalmers, Gothenburg*, ISSN: 1652-8549, 2016.

[D] Jan Anike Nikolajsen, Peter Riddersholm Lauridsen and Lars Damkilde, "The geometric non-linear generalized Brazier effect - a linearized finite element based solution ," *Conference, Proceedings of the 29th Nordic Seminar on Computational Mechanics (NSCM-29), Chalmers, Gothenburg*, ISSN: 1652-8549, 2016.

In addition to the main papers, the following publications have also been made.

[1] Peter Riddersholm Lauridsen, Jan Anike Nikolajsen and Anders Schmidt Kristensen, "Non-linear structural analysis of the folding process in a deployable system for satellites," *Conference, Proceedings of the 30th Nordic Seminar on Computational Mechanics (NSCM-30), DTU, Lyngby*, 2017.

[2] Jan Anike Nikolajsen, Peter Riddersholm Lauridsen and Anders Schmidt Kristensen, "Contact issues on a highly flexible frame for a satellite drag sail," *Conference, Proceedings of the 30th Nordic Seminar on Computational Mechanics (NSCM-30), DTU, Lyngby*, 2017.

[3] Anders Schmidt Kristensen, Jan Anike Nikolajsen and Peter Riddersholm Lauridsen, "Modelling of structural loads in drag augmented space debris removal concepts," *Conference, Proceedings of the 30th Nordic Seminar on Computational Mechanics (NSCM-30), DTU, Lyngby*, 2017.

This thesis has been submitted for assessment in partial fulfillment of the PhD degree. The thesis is based on the submitted or published scientific papers which are listed above. Parts of the papers are used directly or indirectly in the extended summary of the thesis. As part of the assessment, co-author statements have been made available to the assessment committee and are also available at the Faculty. The thesis is not in its present form acceptable for open publication but only in limited and closed circulation as copyright may not be ensured.

Preface

This thesis is submitted in fulfillment of the requirements for the degree of Doctor of Philosophy at the Department of the Build Environment, Aalborg University, Denmark.

The purpose of this dissertation is to introduce other researchers and engineers working with wind turbine blades to new approaches. These new approaches can improve the performance and extend fatigue life of wind turbine blades. Moreover, large structures have always fascinated me, and by the growing demand for wind power, and my background as mechanical engineer this gave a chance to be a part of this journey into a new age of green power.

Denmark has for many years been the leading country regarding research and companies working with wind power, and in order to keep this position, we must keep this momentum. It means that we must minimize the costs of wind energy and make longer and lighter wind turbine blades. To make this possible blades must undergo an optimization process, and I hope my research will contribute to this iterative change.

This PhD project has been carried out at Aalborg University, Esbjerg in the period October 2017 to April 2021 under supervision of Associate Professor Anders Schmidt Kristensen. Personally, it has been motivating and interesting to combine numerical modelling, mathematical models and experimental work.

My ambition with this PhD project is to use my knowledge and experience in the future as researcher, teacher or employee in a company. Moreover, from this PhD project I have learned that research is hard work, and you can not take anything for granted.

Peter Riddersholm Lauridsen
Aalborg University, April 19, 2021

Acknowledgement

I would like to thank the following people for helping with this PhD project:

I will start by thanking my supervisor Anders Schmidt Kristensen for his commitment and his good advise in my period as a PhD student. He has contributed with good suggestions and fine review of both papers and thesis. Moreover, Anders Schmidt Kristensen has been helpful when challenges were demotivating.

A great thanks to my colleagues Jan Anike Nikolajsen and Simon Klinge Nielsen for help and guidance in my study. They have contributed with great ideas and answers every time I have asked. I am also grateful for the laboratory assistance provided by Jan Erland Andersen. He has been friendly every time I have asked for assistance, and he has manufactured several special parts for the experiments.

I appreciate Rasmus Konge Johansen (Polytech A/S, Bramming) for his cooperation, interest in my PhD project and the supply of several test specimens for the experiments.

I also would like to thank Find Mølholt Jensen and Christian Mølholt Jensen from Bladena, to give permission to reuse their figures in this thesis.

A great thanks to Vibeke Brødbæk Hansen for proofreading, corrections and fine comments in this thesis, and at last a special thanks to my wife Mette and my three kids (Caroline, Elise and Carl) for support and encouragement through these 3 years of research.

Part I

Extended summary

Chapter 1

Introduction

This chapter will present the motivation, research hypothesis and problem statement of this thesis, followed by the thesis outline. Moreover, this chapter will cover a brief summary of the historical background behind fracture mechanics and fatigue in structures together with some of the failure modes seen in wind turbine blades. Finally this chapter will present state of the art in this field of research

1.1 Motivation and research hypothesis

Fracture mechanics and fatigue has been intensively studied by researchers and engineers for more than a century, and many of these studies are used for life predictions in structures. The outcome of this research is also used to design more optimal structures in order to increase stiffness to weight ratio. It pushes structures closer to failure limits, and it means that fracture mechanics and fatigue analysis are important fields of research.

Especially the aerospace industry and wind turbine industry are pushing the limits in order to get longer, lighter and stiffer wings/blades [79], and to push these limits is the industry forced to find improved failure theories, simulation methods and test methods. Thereby, is it not only academic interest [53] and curiosity that drives this research but it also has an important purpose in the industry. In addition, there is an understanding in the industry that it is expensive [71] and slow to make tests and interpret the results. Therefore, are improved analysis techniques and test methods requested in order to save time and money. Moreover, composites are becoming more complicated [90], and therefore new approaches and test methods are essential in order to determine and predict the performance of these materials.

The desired probability of failure in a structure is based on many assumptions and the risk of human lives. This can be illustrated by a probabilistic model as the loading

and strength is variable by nature, and the overlap between these is the probability of failure [24] [18]. This overlap is seen in Figure 1.1 where the gray area represent the variation of load and the blue area represent the variation of material strength. If this overlap is too large, it will result in high probability of failure. This can result in costs and loss of human lives which is not acceptable.

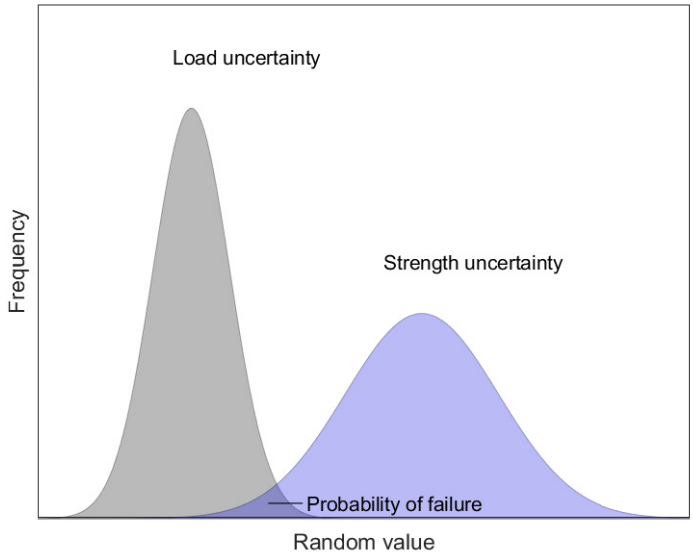

Fig. 1.1: Schematic illustration of the desired probability of failure.

Instead if the probability of failure is very low, it can be concluded that the design is too conservative. This will also result in costs and unnecessary use of material. This is illustrated in Figure 1.2 where the overlap is almost non existing, and this is also not appropriate. Therefore, it will always be to prefer, to find this optimum between the two unintended scenarios.

With added complexity in composites materials it is necessary to develop, improve and optimize test methods in order to identify behavioral parameters accurately and efficiently.. This can be done by developing new test methods that e.g. can be used in the preliminary tests of materials, and this could bring down the uncertainty of strength in laminated composites [76].

Another way to find a design optimum is to use advanced simulation tools, as these are capable of modelling crack initiation and crack propagation in the composite structures. Some of these simulation methods are also used for modelling of imperfections (ply drops, voids), as these can have significant impact on fatigue life in wind turbine blades [60].

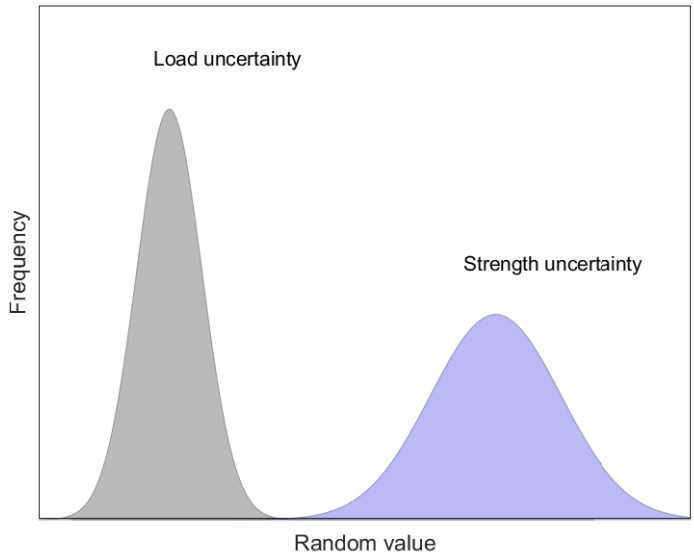

Fig. 1.2: Conservative design of structure as the probability of failure is almost zero.

From the aforementioned observations it can be concluded that fracture mechanics and fatigue still is highly relevant research in the wind turbine industry. It raises the overall scientific question and hypothesis in this PhD project: How is it possible to predict the performance of laminated composites and adhesive joints in slender composite structures with novel methods?

So the main objectives of this PhD project are as follows:

- To obtain a better understanding of failure mechanisms in laminated composites and adhesive joints.
- Development of a novel test fixture that is capable of giving good approximates of fracture resistance in laminated composites and adhesive joints.
- To find an improved test method for determination of mode mixity fracture resistance in laminated composites.
- Development of a simulation tool that is capable approximating additional forces caused by geometric non-linearity in slender composite structures.

1.2 Thesis outline

This thesis is divided into two parts, where part I is an extended summary and part II contains the four papers.

Chapter 1 is the introduction and the chapter starts with motivation, problem statement and scientific question. After the thesis outline is a historical overview of fracture mechanics and fatigue in structures used to underline the importance of research in this field to remind the readers of the risk associated with these phenomenons. The rest of Chapter 1 will describe fundamentals of wind turbine blades, failures and state of the art in testing and designing wind turbine blades. The aforementioned content is used to introduce the reader to the engineering challenges and details in designing modern wind turbine blades.

Chapter 2 focuses on the developed test method (TP-MMB), and details are described in this section. The chapter will start with the scientific contribution and impact of this test method, and afterwards theoretical details will be described and coupled to the TP-MMB test method. This part is followed by a validation test and an experiment with the TP-MMB. Validation of TP-MMB test method is also demonstrated by use of Cohesive Zone Modeling (CZM) in ANSYS software. Finally both pros and cons will be discussed regarding this test method.

Chapter 3 is dedicated to the Finite Element based approaches which can approximate the non-linear force contribution in slender structures. The combination of thin walled cross sections and large deformations of composite structure makes these contributing forces interesting in calculation of fatigue life. Three different types of linearized approaches are described and demonstrated in this chapter. Moreover, the performance of these methods is evaluated.

Chapter 4 will contain concluding remarks and major findings. A discussion regarding future challenges in wind turbine blades will also be to find in this chapter, and after the concluding remarks all references are located.

Part II will as mentioned before contain the four papers, and paper A will relate to Chapter 2. Paper A primarily focuses on the novel concept and validation of the TP-MMB test method.

Paper B, C, and D relates to Chapter 3 and describes three different types of linear approaches to geometric non-linearity. The papers will also demonstrate the accuracy of the linear approaches in Finite Element Analysis of different thin-walled composite structures.

1.3 Historical overview of fracture mechanics and fatigue in structures

Fatigue has been a challenge for engineers for almost 200 years, and back in 1829 was the German mining engineer Wilhelm August Julius Albert the first person to perform fatigue test on conveyor chains and report them [3]. He observed that the numerous failures could not be explained by known theory, and therefore it could only be related to the cyclic loading of the chains.

In 1860 railways were in development and a fatigue problem in wagon axels was observed by the German railway engineer August Wöhler [2]. He observed that the wagon axels were failing frequently and he decided to carry out systematic experiments to find answers to this problem. He constructed a rig where it was possible to control the loading, and count the number of cycles to failure. He found out that the number of cycles to failure depended on the stress level and fatigue failure was probabilistic by nature. He published his experimental work on wagon axels, and he was thereby the inventor of the stress (σ) cycle (N) curves which still is a common tool in today's engineering.

During and after World War I the aeronautical engineer Alan Arnold Griffith was a pioneer in fracture mechanics. He studied fracture mechanics in brittle materials and he found a theoretical relation between crack length, surface energy and elastic energy. These observations and results were in agreement with an energy per unit area criterion, and is best known as surface energy density or strain energy release rate. This criterion applies to all types of cracks and therefore is it still used in today's engineering. His work [33] was published in 1921 and was later on modified by George Rankine Irwin [83].

In World War II Liberty cargo ships were in use by the United States [36]. These ships delivered cargo all over the world and performed as expected under warm conditions. But one night in Portland, Oregon, United States the temperature of the air was relative low and the river was warm. These conditions meant that the ship rapidly and unexpectedly cracked into half. The reason was the brittle welded steel plates, which could not withstand these weather conditions. Engineers were unaware of this problem at this time, and therefore it was not possible to find an answer.

Two tragic aviation accidents happened in 1953 and 1954 and it happened with a specific type of airplane [61]. The accidents happened with an airplane type called Comet. It was the world's first commercial jet airliner made by the de Havilland Aircraft Company. The airplanes were grounded in 1954 because the reason for these accidents was not found. Therefore, a team of engineers and specialists started to build a water tank, where it was possible to test the fuselage. They wanted to perform a fatigue test on the fuselage by pumping water in and out of the water tank. In this way they changed the cabin pressure and it was possible to inspect and analyze the consequences. Their tests showed that cracks started to initiate and propagate near the windows. The reason was stress concentrations and out of plane bending. Therefore, the lesson from

these tragic accidents and experiments was a philosophy that ensured fail-safe designs prospectively.

On April 28, 1988 an airplane was on its way from Hilo to Honolulu in Hawaii [66]. Unfortunately the airplane was forced to perform an emergency landing in Kahului Airport on Maui. The reason for this emergency landing was that a part of the fuselage was imploded. One person died and sixty-five were injured in this catastrophic accident. Shortly after the accident investigators started to inspect the airplane in details and they found significant disbonding and fatigue damage in a lap joint located in the fuselage. The accident report concluded that there were some shortcoming and failures in the maintenance program, and a more detailed maintenance program could have found the fatigue cracking in the fuselage and thereby the accident could have been avoided.

Wind turbines have existed for more than a century and in the last 30 years this industry has grown significantly in size. It has meant that wind turbine blades are getting larger and stiffness to mass ratio has been increased in order to maximize profit. Large wind turbines are capable of harvesting wind power to a lower price, but it has resulted in some challenges. Wind turbines are exposed to challenging weather conditions and it results in varying loads and a high number of fatigue cycles, and when the materials are exploited to the extreme, it will result in failures [59] [94]. It has meant that many of these problems and failures have been studied around the world in order to optimize the performance of wind turbines.

In 2012 cracks in the worlds largest passenger airliner Airbus A380 were also a problem [17]. Mandatory inspections showed that cracks had been found in the wing ribs, and these findings provided a basis for additional inspections on other planes. The European Aviation Safety Agency required that 68 planes in service should undergo an extra inspection, and the planes were selected based on flight hours and load. Cracks were found on at least two planes and the failures were repaired. It was concluded that the cracks came from the manufacturing process and the procedure was changed in order to eliminate the problem.

In 2019 more than 100, C-130 Hercules air-crafts were grounded, and the reason was cracks in the lower center wing joint [56]. If the cracks were not discovered, it could result in a dismantled wing during a flight. The Air Mobility Command took no chances and was immediately in contact with aircraft maintenance and engineers in order to solve the problem. Therefore, the Air Mobility Command ordered extra inspections of the C-130 Hercules, and if the component was damaged, it got repaired.

The historical review has shown that fracture and fatigue in structures have challenged engineers and companies for many years. It is possible to minimize these problems if engineers get a better understanding of how the material fails. It can only happen if materials are extensively tested and new failure criteria are developed. Furthermore, it is still important to have strict manufacturing processes and maintenance programs in order to have reliable performance of structures.

1.4 Wind turbine blade anatomy and loads

Cross section of a wind turbine blade can be constructed in different ways [63]. The reasons for this are many, and one of them is to make it fit into a manufacturing process. In the manufacturing process it can be important to have an efficient production where many blades are produced every day. Another reason for choosing a specific type of cross section, can be the possibility to have a flexible production line, and have a fast change and startup of another blade type.

In Figure 1.3 the most common types of cross sections are illustrated, and if we take a look at the closed shell, it is seen that the load carrying structure is similar to an I-beam. The top and bottom flanges (caps) are designed to withstand the high bending moments flap-wise. The box spar cross section also has the large top and bottom flanges like the closed shell. Moreover, the box spar is having two shear webs instead of one in the closed shell. The last type of cross section is the load carrying shell, and with this design the load bearing materials are primarily distributed near the panels.

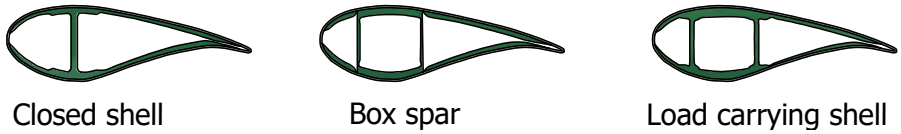

Fig. 1.3: These types of cross sections are primarily used in wind turbine blades.

If we take a look at the details and structural elements of a blade in Figure 1.4, the panels are the outer boundary of the blade. The panels are reinforced on the inside with a sandwich panel and near the spar cap we have an adhesive layer to transfer the aerodynamic loads to the load carrying structure. The load carrying structure is called a main spar and goes from the root of the tip of the blade, and the dimensions of the main spar are customized the blade.

Adhesive joints are seen in the leading and trailing edge. These adhesive joints are necessary as the aerodynamic panels consists of two parts (top and bottom part) and the load carrying structure is one part, and all these are assembled with adhesive joints. These adhesives are made of epoxy resin as these are durable and very strong connections between structural elements. The sandwich panel is often made with a balsa core or foam core (PVC or PET) and bi-axial fibers in the face sheet. The lower part of the panel is called pressure side and the upper part suction side, as this side is generating the lift forces on the blade.

Carbon Fiber Reinforced Polymer (CFRP) and Glass Fiber Reinforced Polymer (GFRP) are commonly used materials in wind turbine blades as these materials are corrosion resistant, stiff, durable, have a high tensile strength and the density is relatively

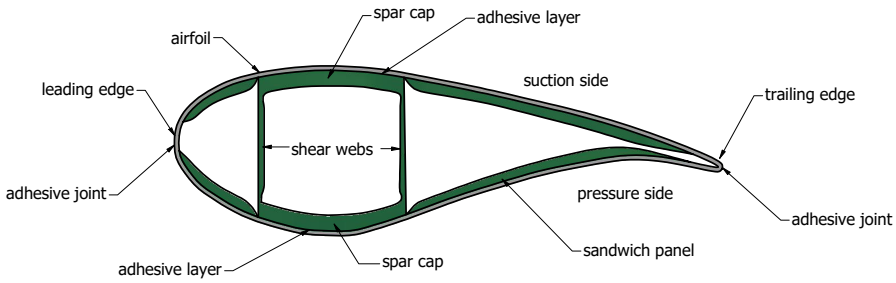

Fig. 1.4: Overview of structural elements in a wind turbine blade.

low. This gives a material with high specific strength and stiffness which is ideal for load carrying components. Moreover, these materials are also used in other segments of the blade as these can be high loaded as well. The fibers are stacked and surrounded by matrix material in order to prevent local buckling and make it a laminated composite. The orientation of the fibres depends on the approximated stress field in the blade, as it is the fiber fabric that primarily carry the loads. In Figure 1.5 the most common used fiber fabrics [91] are illustrated, and if we take a look at the unidirectional fiber fabric these are primarily used in the load carrying element and orientated along the beam axis. The bi-axial fiber fabrics are perfect to withstand pure shear stresses. Therefore, these are used in the shear webs. The last presented type of fabric is tri-axial,and here the fibers are orientated 0°, -45° and 45°. This gives a laminated composite that is designed to resist a changing stress field.

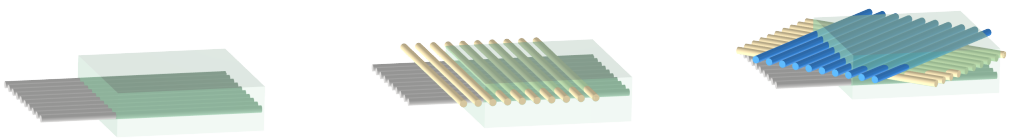

Fig. 1.5: Unidirectional fiber fabric (0°), biax fiber fabric (0°, 90°) and triax fiber fabric (0°, -45°, 45°). The transparent volume illustrates the matrix material.

Wind turbine blades are exposed to many types of loads, and some of the loads are challenging to approximate. If we start with aerodynamic lift, this is increasing towards

the tip of the blade as the velocity of the blade is highest near the tip. Moreover, these forces are constantly changing around the airfoil as the wind is random by nature. The aerodynamic drag is also important as this force pushes the blade towards the tower in an upwind design, and as the blade is slender, this will result in large deformations. Especially wind gusts will result in large deformations and the blade will be close to the tower. To prevent collision between tower and blade in an upwind concept the nacelle is sometimes tilted back over. Another way to prevent collision is to use swept blades, as these are curved unloaded. Moreover, when the rotating blade passes close to the tower the air flow is disrupted, and it will generate a so called tower shadow effect. This will result in unintended noise and vibrations in the blade, which will introduce additional fatigue loads to the blade.

Flapwise loading (F_y) and edgewise loading (F_x) are common used definitions [38] for loads in respectively x-axis and y-axis as shown in Figure 1.6. These types of loads are often combined when testing in order to define a type of loading that is similar to operational loads. Furthermore, if this combined load is offset (L) from the neutral axis of the cross section, it will result in additional torsion. The contribution from torsion is an increasing problem as the blades are getting longer and the deformations are larger.

Besides the aforementioned loads centripetal force and gravitational force are also influential loads, that affects the design of the blade.

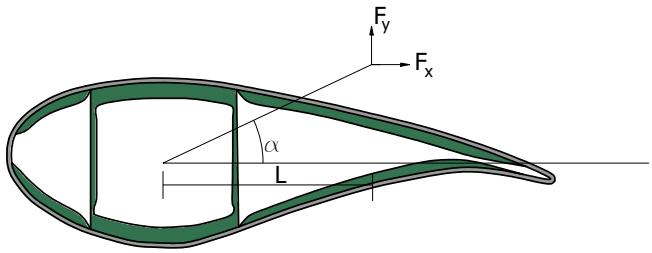

Fig. 1.6: Simplified combined loading of a wind turbine blade which will result in torsion.

It can be concluded that the type of cross section not only depends on getting the stiffest blade and strongest blade with low material consumption, but it must also fit into the manufacturing process where the requirement is high quality and a high number of produced blades every day. It can also be concluded that wind turbine blades are exposed to many types of loads and these are challenging to determine, as the conditions depends on many parameters. This makes it challenging to perform fatigue analysis on wind turbine blades, and there is room for improvement and future work [71].

1.5 Damage, imperfections and manufacturing flaws in wind turbine blades

Wind turbine blades are in general designed with a higher probability of failure than e.g. wings on a airplane or civil engineering structures [89]. The reason for this, is the risk of loss in human lives, which is relative low for wind turbine blades as these are unmanned most of the time. Persons are only close to the wind turbines under construction, maintenance and removal of the turbines. Moreover, these tasks are only performed if weather conditions and other safety rules allow for this. Therefore, this section will show some of the damages, imperfections and manufacturing flaws that can occur in wind turbine blades, as these have an economic interest and safety aspect.

Geometry of a blade is complicated and it results in thickness change of the laminated composites many places. The changes in thickness of the laminated composites give so called ply drops, which are of special interest in a structural analysis. In Figure 1.7 ply drops are illustrated in the transition zone, and between the face sheet and the plies are resin pockets sometimes the problem. These pockets will result in local stress concentrations which can initiate crack growth. Research [75] has shown that it is possible to minimize the size of the resin pockets and it gives a higher load capacity of this detail. The resin is the weak part and prone to crack initiation, especially if this connection contains an imperfection.

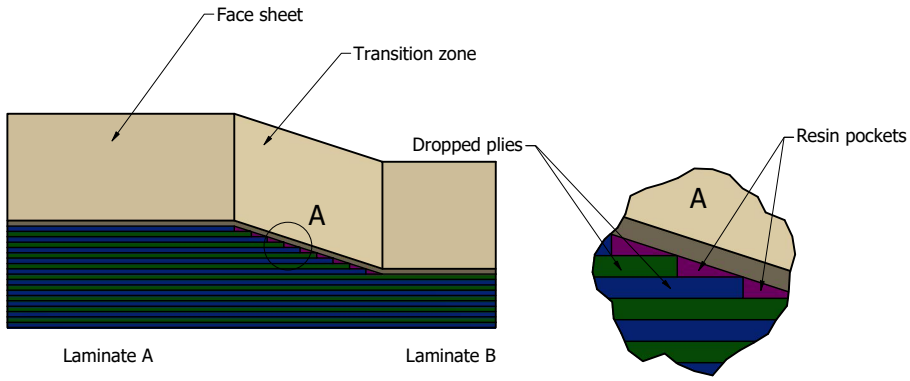

Fig. 1.7: Ply drops are necessary in order to change geometry and get the correct thickness of the laminate in another segment of the blade.

In the manufacturing process are several different types of plies stacked and a vacuum infusion process is used to fill the mould with resin. This is a well known process, and often the challenge is to ensure that resin is all over the mould. If the mould is not filled with resin and fiber, so called voids and delaminations are appearing in the laminated

composite. If we take a look at Figure 1.8 it is easy to identify these manufacturing flaws, as it is possible to see the background through this part several places. The voids and delaminations are perfect conditions for crack initiation and crack propagation as the flaws give stress concentrations and can be assumed to be a precrack. Depending on location of these flaws, these can be surrounded by a low stress field and the flaw will not potential initiate crack growth. If we know the flaws are present by a given density and we know the size of these, it is possible to compensate for this in the design phase. However, this requires extra material in order to lower the overall stresses which could have been avoided if the laminated composite was without these manufacturing flaws.

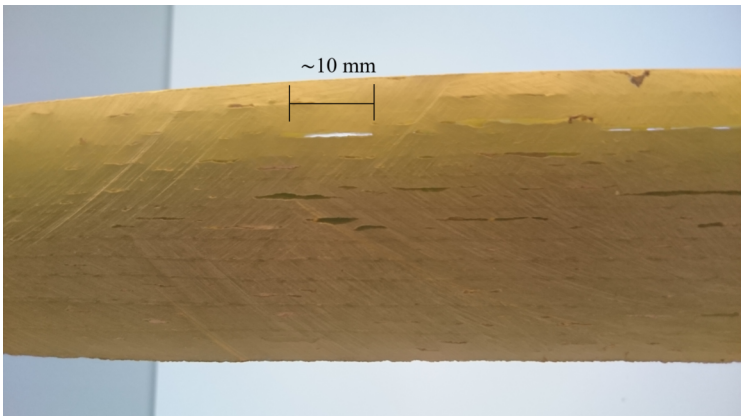

Fig. 1.8: Example of delamination and voids between the plies in the main spar. Through this slice of cross section is it possible to see the background and the distance is approximately 50 mm.

Fibers and matrix material can fail in many ways [92] and some of the most common ways are presented in this section as these failures can provoke other failures and cracks will start and grow trough the structure. If we take a look at Figure 1.9 we see that five examples are illustrated, and failure (A) shows matrix tensile cracking. This type of failure can occur in the manufacturing process and when the composite material is exposed to tension. However, it is also possible to see matrix cracking when the composite is exposed to compression as illustrated in (B). Therefore, a crack path will depend on the load history and the interaction between the stress field in fibers and matrix material. If we take a look at failure (C) this type of failure is often occurring if the fibers are high loaded in tension or the fiber has a local weakness. When a fiber breaks it will result in higher stresses for the nearby fibers and it can result in another breakage. Stress transfer between fiber and matrix can result in fiber matrix shearing failure as illustrated in (D). This type of failure is i.a. governed by the interface strength between fiber and matrix. Therefore, the correct treatment and manufacturing process is important in order to ensure a good attachment between the two materials. This

type of failure can occur in both tension and compression of fiber and matrix. The last failure is depicted in (E) and is buckling of the fibers, and this can only occur if both compression and debonding between matrix and fiber are present. The outcome of this effect can be a significantly drop in load capacity and cracks can also start to propagate.

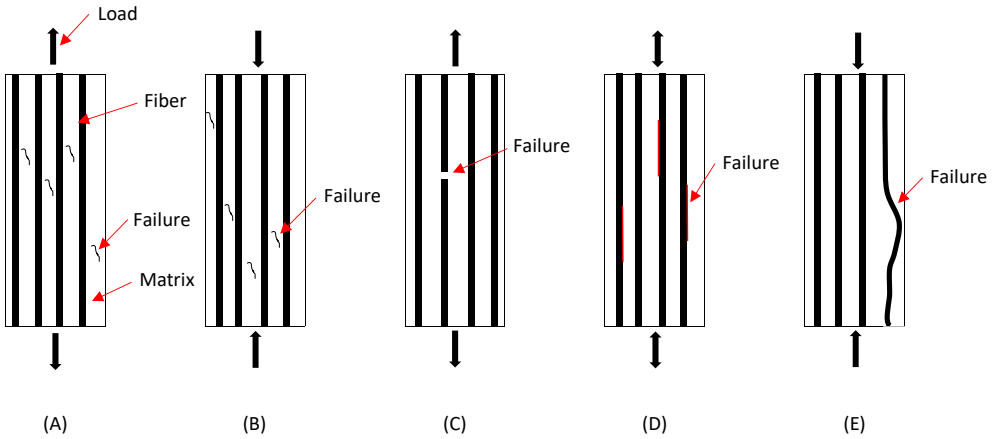

Fig. 1.9: Examples of fiber and matrix failures. (A) Matrix tensile cracking. (B) Matrix compression cracking. (C) Fiber breakage. (D) Fiber matrix shearing. (E) Fiber buckling.

High compression stresses in the panels can trigger local buckling. This is problematic as this causes high stresses in the adhesive joint which is located between the load carrying box spar and the panels. This type of damage is called skin debonding and this type of damage is illustrated in Figure 1.10. It can also be concluded from the figure that this type of damage has significant consequence on the structural performance. The skin debonding is caused by so called peeling stresses and these are not only related to buckling as these also occur when the blade is normally loaded. Peeling is an effect that appear in the interface between the adhesive and the first layer of fabric in this case. However, the problem with buckling is that stress intensity can be so high near the crack tip that it exceeds the fracture resistance of the adhesive joint. Moreover, the problem with initiation of skin debonding, is also caused by the change in geometry as this gives stress concentrations. Peeling can also appear in the leading or trailing edge as the blade can be exposed to an effect called breathing. This effect causes the upper and lower sandwich panels to move against and away from each other. This is similar to two loads pointing in opposite directions and the crack will have the perfect conditions to start propagating. This phenomenon is illustrated in Figure 1.11, and the crack is clearly seen in the trailing edge.

Weather conditions like temperature have a clear impact on the mechanical properties in laminated composites, and thereby the frequency of damages in blades. Fracture

Fig. 1.10: Buckling can cause high peeling stresses and thereby skin debonding. Adapted with permission from Find Mølholt Jensen, Bladena.

toughness will decrease as the temperature drops and if the loads are relatively high it will result in several damages in a short time. Research [58] [43] has shown how temperature can influence on fracture resistance and damages, and the results showed that fracture resistance in CFRP was significantly reduced when the temperature was -30 °C. This type of environmental testing is also possible with the TP-MMB test method, as all parts of this test fixture can withstand these low temperatures.

These low temperatures are present at some locations where wind turbines are operating, and therefore important to take into account. The low temperatures in combination with e.g. non-linear geometric effects or wind gusts can result in a breakdown of the wind turbine.

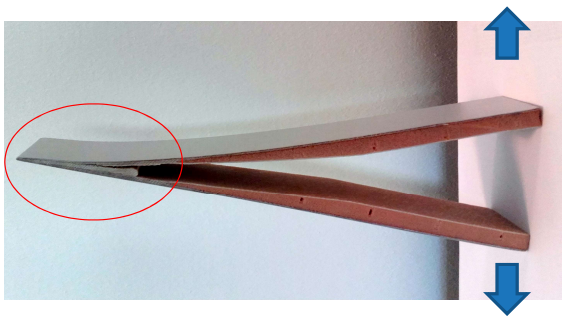

Fig. 1.11: High peeling stresses in the trailing edge. Adapted with permission from Find Mølholt Jensen, Bladena.

When a blade contains either imperfections, damages or manufacturing flaws the probability of a breakdown is high, and in worst case scenario parts of the blade will fall of. In Figure 1.12 the shell is disbonded from the box spar, and an inspection of the image shows large and many voids in the adhesive layer. This is definitely a manufacturing flaw that introduced a poor bonding between the box spar and the shell. The crack growth rate in a blade will depend on the load history and the number failures, and in a blade like this with many voids fatigue life is reduced significantly.

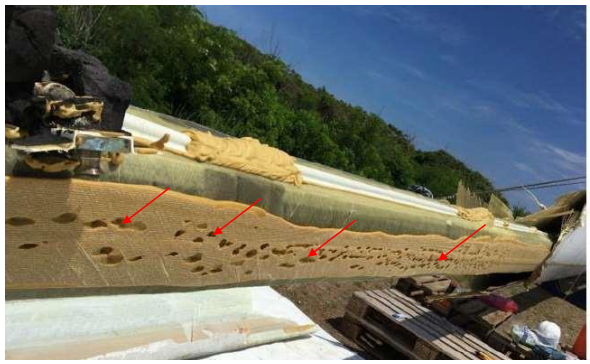

Fig. 1.12: Shell disbonding from box spar. The red arrows indicate where some of the voids are located in the adhesive layer. Adapted with permission from Find Mølholt Jensen, Bladena.

Under the right circumstances a so called flutter effect can appear in the blade. This effect is an interaction between the eigenfrequencies of the structure and the aerodynamic forces. This effect introduces vibrations and mechanical resonance which is damaging for the structure, as local stress levels can exceed the maximum tensile strength of the material and the crack will start to propagate.

A high flapwise bending moment can lead to buckling in the blade. Especially in the segment where the blade has a long chord length and the compressive stresses are high. The trailing edge region is especially prone to buckling and the outcome can be a delamination in the trailing edge. However, the opposite can also be a problem, as delamination will influence on local buckling in the blade. Research [39] has concluded that delamination can induce local buckling modes in the blade, and these can appear below the design load level.

Some of the aforementioned damages can be caused by Brazier effect [9] in the blades, as this phenomenon induce contributing forces in the blade and thereby stresses. This effect is a part of this thesis and will be further explained in Chapter 3.

This section has shown that damages, imperfections and manufacturing flaws are well known challenges that have to be considered and minimized in order to get the best blade performance. Therefore, requirements for new simulation tools and test methods are sought to address these problems, and thereby prevent breakdown.

1.6 State of the art for testing and designing wind turbine blades

Structural testing of laminate composites and adhesive joints are important in order to know the performance and the limitations of these materials. Mechanical properties like yield strength, Young's modulus, maximum tensile strength, fracture toughness, crack growth rate and fatigue strength are some of the essential parameters that are sought in order to optimize the structural performance.

Structural testing can be divided into specific categories, dependent on the test purpose. Therefore, some of these are listed below and each type of testing is explained in the following text:

- Coupon testing
- Temperature testing
- Subcomponent testing
- Component testing
- Full scale testing

Coupon testing are small test specimens with a size of e.g. 300 mm in length, 20 mm in width and 15 mm in height. These types of tests are typically used for quality control of incoming batches used in a manufacturing process. These types of tests can give a representative result on the failure mechanisms like fracture toughness, and the batch can either be accepted or rejected. An example of coupon testing can be a specific ASTM standard [1] where the purpose is to determine the fracture toughness in unidirectional fiber reinforced polymer matrix composite. This type of test is performed in a standard tensile testing machine with a special designed test fixture that fit into this machine. The test fixture is capable to apply the required loads in such a way that the specific mode mixity is obtained.

Researchers have performed fatigue testing on small test specimens in laminated composites, and some examples are given here [35] [98] [30] [76]. These types of fatigue tests are not necessarily following any standards, and are instead dealing with specific research questions. Fatigue testing with small test specimens are important in order to find fundamental mechanical properties, and be able to predict the performance in larger components or structures.

Materials test at different temperatures is a well known type of test and an example would be determination of fatigue strength [62]. However, this type of test is important to perform in order to get the mechanical properties at different temperature ranges. Temperature testing is typically performed on coupons and subcomponent as it requires an environmental chamber to perform. Temperature testing on adhesive joints is also

common, and stiffness and strength will reduce when temperature is increasing as it was demonstrated by Nguyen et. al. [69].

Subcomponent testing of wind turbine blades can be required in a certification process [23] or academic research [54] [4] [29] [5]. If fiber orientation and location are interrupted by multiple layer overlap this will have an impact on the structural performance. Therefore, verification of specific components are required. In addition, this type of test is also useful if crack growth rate and crack growth direction is investigated. Subcomponent testing of the trailing edge has also been demonstrated by Rosemeier et. al. [82], and they have developed a novel concept of testing subcomponents which follows new standards and guidelines.

Component testing or segment testing of wind turbine blades can for example be used to determine buckling loads. Buckling is often occurring in areas where the blade has a long chord length, and only the segment between the root and the midspan is needed to perform such a test. Buckling will often occur in the panels near the trailing edge.

Full scale structural testing of wind turbine blades is often the final test in order to get the design verification, and the test procedure, interpretation and evaluation of results can follow the IEC 61400-23:2014 standard [42]. Both fatigue testing and static testing are performed in such a process and this type of test is known to be expensive and time consuming. The timespan can be 6 months in order to prove an accelerated performance test and fatigue test of the blade. Thereby, this type of test is important for the manufacturing company.

The number studies and findings from academic research in laminated composites and adhesive joints are countless. Both experimental studies and development of numerical simulation tools for prediction of crack growth rate and direction are to find in many papers. If we start with some of the experimental research a test method developed by Bent F. Sørensen [88] is useful in order to determine the fracture resistance in both laminates, adhesives and laminate/adhesive interfaces. The special test rig is able to generate pure bending moments to each of the two beams in a Double Cantilever Beam (DCB) specimen, and it is possible to change direction and ratio between the applied moments. It means that it is possible to test the full range in between fracture mode I and fracture mode II. This test method was also used by Jeppe B. Jørgensen [50] to determine tunneling crack growth rates in adhesive bonded joints. It can be concluded from his study that this test method was able to provide stable test results. Moreover, this test rig was developed by Bent F. Sørensen and used by Jeppe B. Jørgensen in his research, and this is an expansion of the research provided by Hutchinson and Suo [41].

Hutchinson and Suo developed a general solution for this problem, and demonstrated the many possibilities with this mathematical model. They also mentioned that their solution can be derived from the J-integral developed by Cherepanov [15] and Rice [80] independently. The TP-MMB test method presented in this PhD project has also used the advantages of the general solution developed by Hutchinson and Suo, and this will

be elaborated in Chapter 2.

Brunner, Blackman, Davies et. al. have also shown novel research [11] [20] [21] in the field of fatigue and fracture mechanics. They have demonstrated different types of test methods/procedures and proposed different test parameters in order to get better estimates of fracture toughness and crack growth rate. Most of their research has focused on experimental challenges and ideas to handle these, and come up with a higher accuracy of the results.

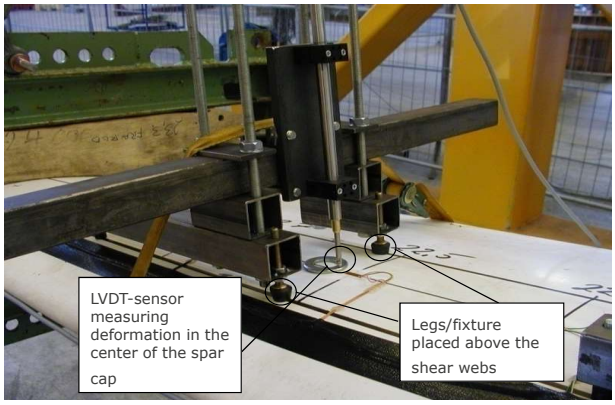

Fig. 1.13: Test of the Brazier effect on a box bar. Adapted with permission from Find Mølholt Jensen, Bladena.

Find Mølholt Jensen has performed tests with wind turbine blades and analyzed the different effects that can occur [46]. Analysis of mechanisms like buckling and the Brazier effect [49] are some of the most import findings in his research. In Figure 1.13 some of his experimental work is illustrated, and the purpose of this specific test was to measure the deformation of the spar cap. This local deformation is caused by the geometric non-linearity, and to be more specific the Brazier effect. This effect gets more pronounced when a blade is exposed to high bending moments and high curvature. The problem with this effect is that it gives high stresses in the corners between the spar cap and shear webs, see Figure 1.4.

To prevent damages from the Brazier effect and other effects in wind turbine blades Find Mølholt Jensen and Bladena have come up with different types of solutions. These solutions are different types of stiffeners which reduce the local deformation of the cross section and thereby avoid crack propagation in the blade. If we take a look at D-strings®, these are designed to eliminate the so called breathing effect, as this effect causes the panels to oscillate. This effect can lead to high peeling stresses and cause crack propagation in bond lines. The D-String solution is shown in Figure 1.14.

X-stiffener^{TM}is another solution which increases the rigidity of the cross section.

This solution is mounted in the box girder corners and the wires goes from one corner to the opposite corner. It results in two wires which prevent large deformations of the box girder cross section. The X-stiffener^{TM}can prevent some of the deformations caused by the Brazier effect, as this effect can cause distortion or skewness of the cross section. Both D-strings® and X-stiffeners^{TM}can be installed when the blade i new or used later for repair.

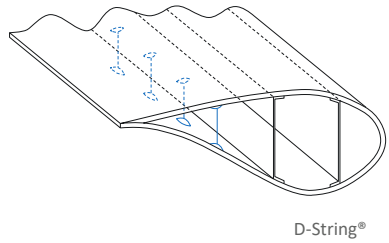

Fig. 1.14: D-string patent developed by Bladena. Adapted with permission from Find Mølholt Jensen, Bladena.

In Figure 1.15 a crack is repaired with the D-string® solution. The picture shows a repaired crack perpendicular to the beam axis, and the blade is reinforced with the D-strings® solution.

Fig. 1.15: Crack in panel repaired with D-string solution. Adapted with permission from Find Mølholt Jensen, Bladena.

Numerical studies on the effect of delamination on local buckling has been studied by Haselbach et.al. [39]. This research proved that even small areas of delamination could lead to local buckling which resulted in crack propagation even under normal load conditions. This study concludes that delamination near the surface can be critical in the main spar. They also mentioned that the Brazier effect [9] had a significant influence on the stress field surrounding the area of delamination. The so called Brazier effect will be elaborated in Chapter 3 where the Finite Element based approaches to this non-

linear effect will be presented. Geometrical nonlinearity in wind turbine blades has also been studied by other researchers [100] [40] [16] [101], and it can be concluded that this effect is of special interest as it entails new failures.

Research delivered by Brian Bak et.al. [6] has shown that cohesive elements can be used for fatigue simulations, as these new elements are able to handle crack growth rate. The elements are defined by a traction separation law and a damage parameter is introduced. This damage parameter depends implicit on the near crack front stress field and it result in a change of the traction separation law. It can be concluded that this is an effective way to simulate crack growth in composite structures.

Esben Lindgaard et. al. [55] has developed a cohesive element which performs with good accuracy and the rate of convergence is faster compared with other formulations of cohesive elements. Sometimes the traditional cohesive elements are faster to converge and it depends on the assigned parameters. This advantage provides the opportunity to have a better discretization of the model or have a faster solution.

Laura Carreras et. al. [13] has developed models for simulating 3D crack growth in composites both under quasi-static and fatigue loading. They presented implementation of six different methods in cohesive elements and these were aimed for high-cycle fatigue. The performance of these methods was varying and only the method developed by Brian Bak et. al. [7] showed high accuracy and robustness.

The technique eXtended Finite Element Method (X-FEM) was proposed back in 1999, and as the name explains it is an extended formulation to the shape functions used in traditional Finite Element formulations. This technique is especially suitable for strong discontinuities like cracks, as the stress field near the crack tip is well defined with X-FEM. However, there are some drawbacks with this method and it comes from the so called blended elements which gives less good approximations of the stress field. The blended elements are located in the field near the crack path and these are mixed with traditional elements which gives less good approximation of the stress field. It can be concluded that X-FEM has potential to be even more efficient for crack simulations if this technique is refined. More details about X-FEM can be found in this literature: [64] [22] [51].

To bring down computational time has beam model approaches also been developed [65], and these approaches are in some extent able to describe the geometric nonlinearity in wind turbine blades. However, these methods also have limitations and the presented method can in some extent address these challenges.

Gradient based optimization of wind turbine blades [85] [86] [57] is also state of the art research in order to fulfill the general light weight requirement. These algorithms also require good approximation of stress field, as orientation of the fibers depends on these. It means that geometric nonlinearity also will have an influence on the outcome of the optimization process if these are included.

There are still many unanswered questions that need to be answered in fracture mechanics and fatigue in composites, and these answers will benefit future work and prevent failures. This subsection has described some of the important findings in this field of research that relate to this thesis and many more are to be found in the literature.

Chapter 2

The Two Point Mixed Mode Bending (TP-MMB) test method

This chapter is based on paper A and theory related to the presented test method. Moreover, the experimental work with uni-directional laminated composites and a Finite Element simulation of the delamination process is described in this chapter. Some of the material in this chapter is adapted with permission from SAGE Journals.

2.1 Scientific contribution and impact

The primary contribution with the presented Two Point Mixed Mode Bending (TP-MMB) test method is to provide a new solution to a known challenge. The challenge is determination of fracture resistance in laminated composites and adhesive joints, as existing test methods have different advantages and disadvantages, and to mention a drawback then compliance calibration is one of them. The calibration is often inaccurate [20], and the TP-MMB test method does not need compliance calibration in order to determine fracture resistance.

The TP-MMB test fixture is developed to be a stand alone apparatus, which fits into a standard tensile testing machine and changing the set up is simple. The main feature of the TP-MMB is the utilization of symmetry in a Four Point Bend (FPB) [21], as this test method only requires half the size of the test specimens. An advantage with eliminating one of the two crack fronts is to have the pure force displacement response from only one crack front when the test is performed. Moreover, the TP-MMB test fixture can also fit into an environmental chamber if influence of temperature on

fracture resistance is studied.

With this test method the mathematical operations are simple in order to determine fracture toughness. Furthermore, scaling the test method is also a possibility if size effects have a significant impact on the fracture toughness.

The TP-MMB test method is able to determine fracture toughness even though large scale fiber bridging appears in the test specimen during a test. This is a challenge for many other test methods as these depend on a well defined crack front to specify a precise crack length. This is one of the pros with this test method as long the fracture process zone will appear in the defined interlaminar interface.

Some test methods are designed to determine fracture resistance for either pure mode I or pure mode II. This means that the non-linear behaviour in between is almost unknown as only few test methods are able to handle this range. Therefore, novel methods are sought, as mixed fracture modes are more realistic in structures exposed to fatigue loads. The TP-MMB determines fracture resistance at a specific phase angle (ψ) which lies in between fracture mode I and fracture mode II. The specific phase angle is 41° for both TP-MMB and FPB. Some of the most common test methods are listed below and illustrated in Figure 2.1.

- $\psi =$ 0° - Double Cantilever Beam (DCB)
- $\psi = 41°$ - Two Point Mixed Mode Bending (TP-MMB), Four Point Bend (FPB)
- $\psi = 90°$ - End Notch Flexure (ENF), End Loaded Split (ELS)

The test fixture can be modified in such a way that if horizontal forces are applied to the test specimen the phase angle will increase. It means that this modification will give a phase angle range from 41° to 90°. This modification will make the test fixture more versatile and be a new and interesting way to test fracture resistance.

2.2 Theoretical background to elastic fracture mechanics

The theoretical background is based on linear elasticity as the zone of plasticity near the crack tip is assumed to be very small compared to the size of crack length, and thus assessed negligible. This theory is among many others described in following literature [95], [34], [77], [10], [31] and [102].

As linear elasticity is assumed near the crack tip, it is possible to apply the advantages of the Stress Intensity Factor (K) developed by Irwin [45] [83] as this factor can be used as failure criteria for crack propagation. This approach was originally derived by H. M. Westergaard [99] who developed a stress function which was able to describe the stress field near the crack tip. His solution was based on the solution from Inglis [44].

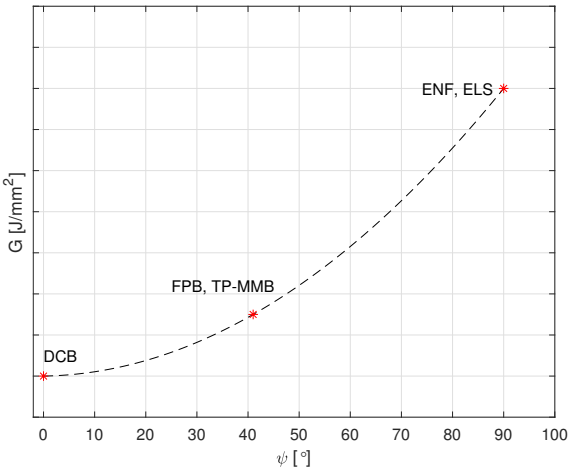

Fig. 2.1: Schematic illustration of the non-linear relationship between phase angle and energy release rate. The different test methods are designed to determine the energy release rate at specific phase angles.

If we go back to Irwin's solution it was based on an infinite plate with a crack length of 2a. This crack was not elliptical and the plate was subjected to a uniform stress state around the crack. Figure 2.2 illustrates the finite cracked plate where the stress field is approximated near the crack tip with use of Eq. 2.1-2.3. The position is described in polar coordinates.

$$\sigma_x = \frac{\sigma\sqrt{\pi a}}{\sqrt{2\pi r}} \cos\frac{\theta}{2}\left(1 - \sin\frac{\theta}{2}\sin\frac{3\theta}{2}\right) \tag{2.1}$$

$$\sigma_y = \frac{\sigma\sqrt{\pi a}}{\sqrt{2\pi r}} \cos\frac{\theta}{2}\left(1 + \sin\frac{\theta}{2}\sin\frac{3\theta}{2}\right) \tag{2.2}$$

$$\tau_{xy} = \frac{\sigma\sqrt{\pi a}}{\sqrt{2\pi r}} \cos\frac{\theta}{2}\sin\frac{\theta}{2}\cos\frac{3\theta}{2} \tag{2.3}$$

These analytical definitions are fundamental in fracture mechanics and the fracture mode Stress Intensity Factor i directly connected to the energy release rate (G) by this formula:

$$G_I = \frac{K_I^2}{E}, \quad G_{II} = \frac{K_{II}^2}{E} \tag{2.4}$$

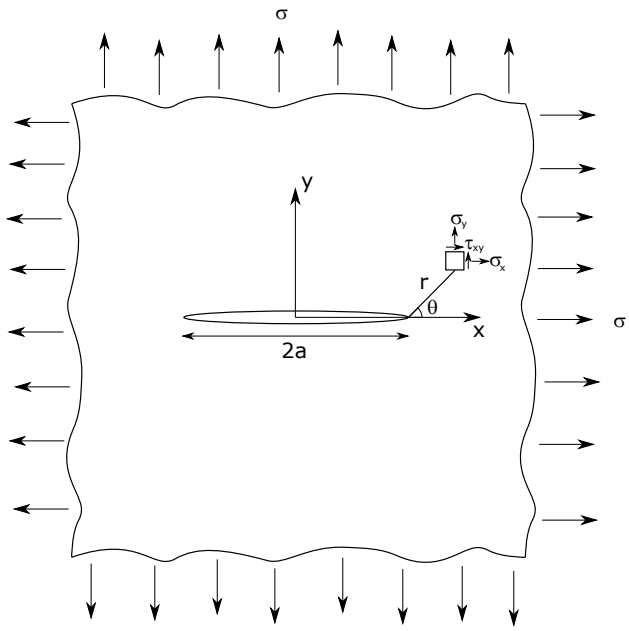

Fig. 2.2: Infinite plate subjected to uniform stress and with a finite crack length of 2a.

The aforementioned strain energy release rate can also be expressed with the J-integral developed by Cherepanov [15] and Rice [80] independently. This method is path independent and an advantage when fiber bridging occurs as the path can cover this long process zone. If the path (Γ) is not closed, the J-integral is non-zero and equivalent to the strain energy release rate. Rice proved his theory on some of his earlier publications [81] and theory presented by Neuber [68].

Figure 2.3 illustrates how the contour path integral can cover the crack tip, and where the traction vector (t) is evaluated with use of the normal vector (n) and the stresses (σ) along the path. If we take a look at Eq. 2.5 the strain energy density (W) is integrated in x or y direction and the aforementioned part is subtracted as this represents the strain energy release rate.

$$J = \int_\Gamma \left(W dy - t_i \frac{\partial u_i}{\partial x} ds \right) \tag{2.5}$$

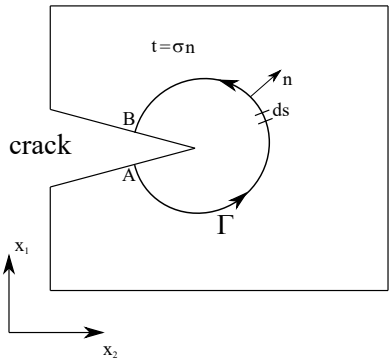

Fig. 2.3: Illustration of a two-dimensional evaluation of the J-integral.

To understand Griffith's [33] and Irwin's theory [45], we start with the term dissipated energy (Ω) or loss of elastic energy during a fracture test where forces and displacements are measured. The dissipated energy is equivalent to the difference between the amount of used energy and the remaining elastic energy. This is illustrated in Figure 2.4 where the the crack length a_1 is increased and gives a reduction of stiffness. Thereby, the relation between dissipated and increase in the crack area is equivalent to the fracture resistance. This can also be proved as the compliance increase when the crack increase in length [104] [103].

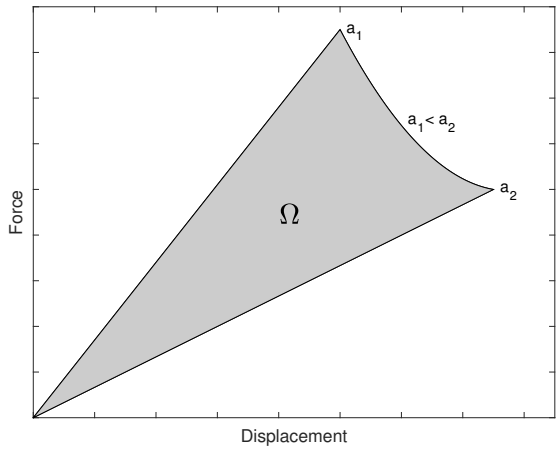

Fig. 2.4: Schematic illustration of the relation between change of crack length and dissipated energy.

Hutchinson and Suo [41] derived a solution from the theory presented by Rice [80] as they demonstrated two special configurations. One configuration where pure bending was applied two beam like arms, also known as Double Cantilever Beam (DCB), and the other configuration where constant displacement was applied to the upper and lower part of the DCB specimen. These configurations and the theory by Rice helped Hutchinson and Suo to find a general solution that could be used for practical use.

The general solution for energy release rate (G) by Hutchinson and Suo is shown in Eq. 2.6 and the parameters related to this solution are found in Eq. 2.7 and Figure 2.5. If we start with the effective modulus of elasticity ($\overline{E}$), this will depend on Poisson's ratio (ν) and plane stress or plane strain conditions in the test specimen. Furthermore, the area moment of inertia is only defined by height of the upper beam (h) and lower beam (H) as the applied bending moments (M_n) and/or forces (P_n) are defined per unit width.

General solution:

$$G = \frac{1}{2\overline{E}} \left(\frac{P_1^2}{h} + 12\frac{M_1^2}{h^3} + \frac{P_2^2}{H} + 12\frac{M_2^2}{H^3} - \frac{P_3^2}{h+H} - 12\frac{M_3^2}{(h+H)^3} \right) \tag{2.6}$$

The effective Young's modulus:

$$\overline{E} = \frac{E}{1-\nu^2} \quad (Plane\ strain), \quad \overline{E} = E \quad (Plane\ stress) \tag{2.7}$$

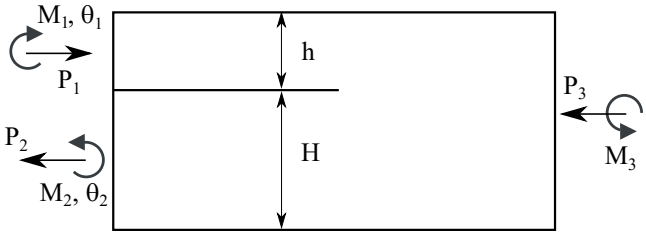

Fig. 2.5: DCB specimen loaded with bending moments and axial forces per unit width.

If we slightly ramp two different bending moments to respectively the upper and lower beam, these will at some point remain constant as shown in Figure 2.6, and at this plateau is it possible to determine the strain energy release rate with Eq. 2.6.

Due to the special configuration of the TP-MMB is the phase angle (ψ) fixed to 41°, as the pure bending moment is only applied to the lower beam. The phase angle is expressed as inverse tangent function to the ratio between the Stress Intensity Factors (SIF) for respectively fracture mode I and fracture mode II. This also can be expressed by the ratio of the applied bending moments and this is seen in Eq. 2.8.

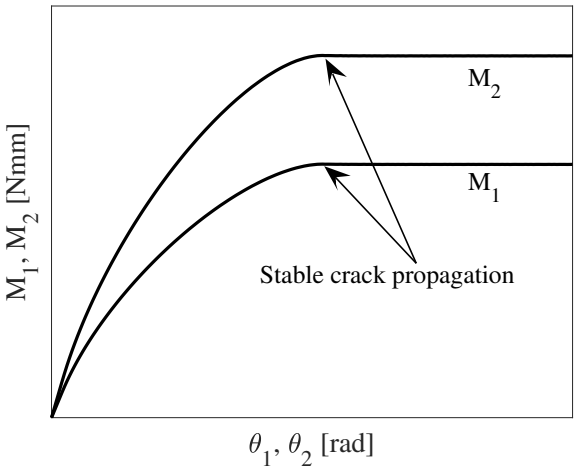

Fig. 2.6: Schematic illustration of a moment-angle curve.

Mode mixity/phase angle:

$$\psi = tan^{-1}\frac{K_{II}}{K_I} = tan^{-1}\left[\frac{\sqrt{3}}{2}\frac{M_1 + M_2}{M_2 - M_1}\right] \approx 41°, |M_1| < M_2 \tag{2.8}$$

The TP-MMB is designed to apply only pure bending to the lower beam in a DCB specimen, it means that Eq. 2.6 can be reduced and only four parameters are needed to determine the energy release rate.

Reduced solution:

$$G = \frac{M_2^2}{\overline{E}}\left(\frac{6}{H^3} - \frac{6}{(h+H)^3}\right) \tag{2.9}$$

The aforementioned theory describes primarily the mathematical solutions which can be applied to the TP-MMB test method and the next subsection will describe the functionalities of the test rig which fulfill these conditions.

2.3 Introduction to the TP-MMB test method

The Two Point Mixed Mode Bending (TP-MMB) test method is a new approach to an already known problem, as the TP-MMB test method is inspired by the independent developed test methods by Charalambides [14], Plausinis [78] and Sørensen [88]. However, the TB-MMB still differ from the aforementioned methods as this concept is a stand alone test fixture which is versatile and relative simple to use.

The TP-MMB test method can also be used for determination of fracture resistance in bi-materials [28] with simple modifications of the governing equations. This type of test is illustrated in Figure 2.7 where two substrates with an adhesive layer in between is exposed to pure bending by the TP-MMB test method. In order to find the fracture resistance of bi-material interfaces must the general solution by Hutchinson and Suo be modified [93], and this has also been demonstrated by Sørensen [87].

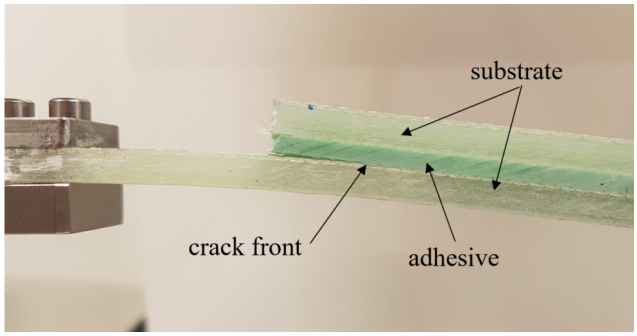

Fig. 2.7: The TP-MMB test method can also be used for determination of adhesive fracture resistance.

The solution to this bi-material problem is shown in Eq. 2.10-2.13 where the adhesive layer thickness (H_a) and substrate thickness (H) are some of the parameters. Moreover, are Poisson ratio and Young's modulus for respectively substrate (E_2, v_2) and adhesive (E_1, v_1) included in order to find the dimensionless parameters (I_1, η, Σ) which compensate for offset in the neutral axis. Test specimen width (W) and the pure bending moment applied the lower beam (M_2) are also included in order to determine the energy release rate (G).

$$J = G = \frac{1}{W^2 H^3 E_2}\left(6M_2^2 - \frac{M_2^2}{2\eta^3 I_1}\right) \tag{2.10}$$

$$I_1 = \frac{1}{12}\left(\Sigma + \frac{8}{\eta^3}\frac{12}{\eta^2} + \frac{6}{\eta}\right) \tag{2.11}$$

$$\Sigma = \frac{E_1\left(1-v_2^2\right)}{E_2\left(1-v_1^2\right)} \tag{2.12}$$

$$\eta = \frac{H_a}{H} \tag{2.13}$$

The test fixture consists of different functionalities and these will be described, and many considerations have been made to come with this specific solution. If we take a look at Figure 2.8 the test fixture consist of a base which is bolted to the tensile testing machine. In this case the test fixture is designed to fit a MTS 858 Table Top tensile testing machine.

In Figure 2.8 it is also seen that the test fixture is equipped with three supports. Support(A) is designed to absorb the pure bending moment applied to the lower beam in a Double Cantilever Beam (DCB) specimen. Support(A) consists of a clamping mechanism with two bolts which ensure good contact between test specimen and support. This support is connected to a slider which allow for a vertical displacement of support(A). The slider is guided by eight roller bearings which is pretensioned with four compression springs in order to ensure full contact between roller bearings and slider, as shown in Figure 2.8. In order to minimize the weight of the slider on the measured results is a counterweight connected to keep it in balance. Moreover, the slider has a stroke of 90 mm in order to handle flexible test specimens.

Support(B) is attached to the crosshead of the tensile testing machine, and this support consist of a round bar supported by two roller bearings in order to minimize the rolling resistance. In this support are both force and the vertical displacement measured, as the force i used for determination of the fracture resistance.

Between support(B) and support(C) the distance is 185 mm (L = 185mm), and this distance is used to generate the pure bending moment. This support is also constructed with a round bar attached to two roller bearings, and this support is connected to the base.

Support(A) is equivalent to the symmetry line in a four point bend and this test method uses this symmetry line to have only one crack in the test specimen instead of two cracks. There are methods to fix one of the two cracks in a Four Point Bend (FPB). However, it does not make sense to have a large test specimen if half of the size is enough. Therefore, the type of specimen used in TP-MMB is with only one crack front, as this gives a more clear response of the measured forces.

In order to verify both test method and test fixture is a special test performed with the TP-MMB. In this case a special manufactured test specimen was used to have a controlled crack front. The special test specimen was made of aluminium alloy in favor of having a homogeneous material, in which it was possible manual to change the crack length (a).

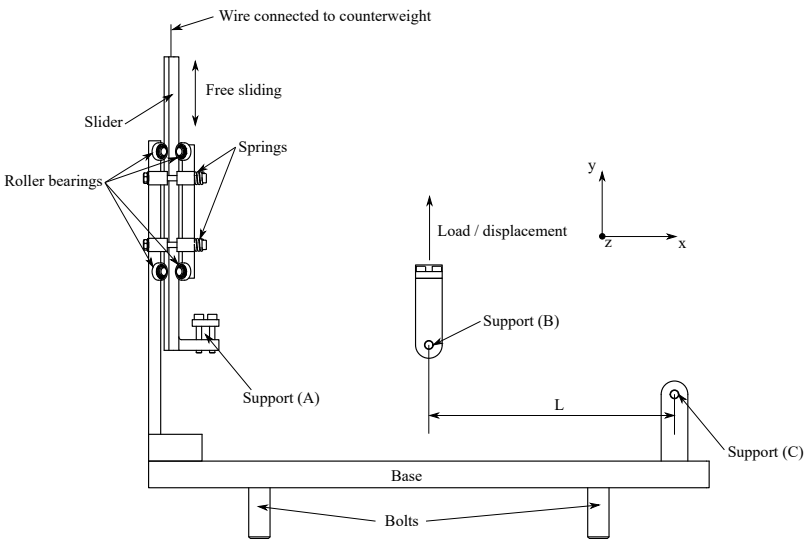

Fig. 2.8: Diagram of the TP-MMB test fixture.

Before this test the modulus of elasticity was determined in a separate three point bending test on the same batch of aluminium alloy bars. This test was performed on the same tensile testing machine, and the result was a Young's modulus equivalent to 66,000 MPa. It can be discussed if this seems to be a low value and the Young's modulus should be higher. However, primarily plane stress conditions are presented as the test specimen is relatively small and this will reduce the stiffness.

The test specimen is 20.0 mm in width (W) and the total height of the test specimen is 8.0 mm (H+h), and to emulate a crack some of the upper part of the test specimen was removed. Removing some of the material was performed in a milling process, and this means that the upper beam was completely removed and the height of the lower beam was reduced to 5.5 mm (H). The special test specimen is illustrated in Figure 2.10 and a length corresponding to the crack length was removed.

The aluminium alloy test specimen was processed two times to emulate two different crack lengths. The first crack length was 28.8 mm and the second crack length was processed to be 128.8 mm.

A quasi-static displacement controlled test was performed with a displacement rate on 0-4 mm/min of the crosshead. Two cycles were performed in order to have a stable measurement and to ensure that local plasticity near the crack tip was constant. Local plasticity near the crack tip is unavoidable as the sharp corner caused by the milling process will introduce this zone. The displacement of the crosshead was fitted in such a way that the measured forces just precisely exceeded 100 N.

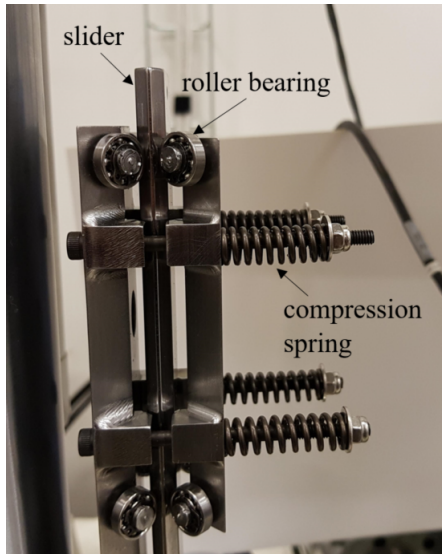

Fig. 2.9: Pretension and guidance of slider with roller bearings and compression springs.

As compliance gets higher when the crack length increases this will result in a change of strain energy in the test specimen. This change of energy can be considered as the amount of dissipated energy caused by a fracture process. It means that an arbitrary horizontal line can be used, as this fulfills the criteria by Hutchinson and Suo and the plateau shown in Figure 2.6.

To fit the two force displacement curves for respectively a=28.40 mm and a=128.80 mm, are quadratic polynomials used. The polynomial fits are illustrated in Figure 2.11 with a 95% confidence interval (dashed lines). A reduction of data has been performed near the starting point, as these data points were interrupted by contact and pretension of test specimen and supports.

The amount of dissipated energy (Ω) was estimated to be 668 mJ and the change of fracture area (A) is measured to be 2008 mm^2. This gives an energy release rate corresponding to 0.333 mJ/mm^2. This is higher than the analytical solution as expected, as the analytical solution gives results on 0.316 mJ/mm^2. This results in a relative error on 5.6 % which is acceptable because some uncertainties can interrupt this result. An overview of results are shown in Table 2.1.

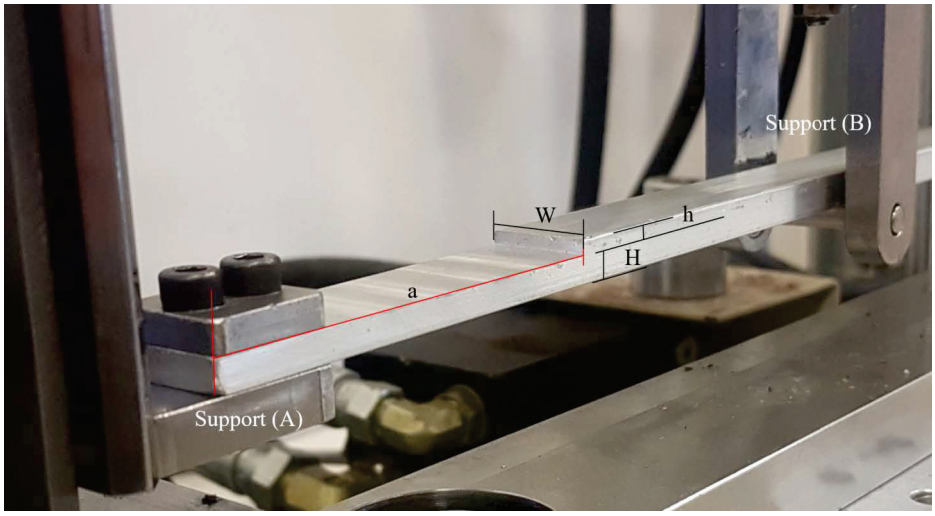

Fig. 2.10: Test set up with validation test specimen (Aluminium alloy bar EN AW-6082 T6) (a = 128.80 mm).

Table 2.1: Overview of measured and calculated results.

A	Ω	$G_{experiment}$	$G_{analytical}$	Error
2008 mm^2	668 mJ	0.333 mJ/mm^2	0.316 mJ/mm^2	5.6 %

Some of the relative error can be explained by the clamping mechanism in support(A), as the test specimen has been unmounted and mounted again. This can introduce a change of compliance in support(A), and introduce an error. Furthermore, the rolling resistance between the slider and the roller bearings will result in dissipated energy, and the two strokes are different which will interrupt the results. This effect should minimize the error and must be further investigated. So, changing the counterweight connected to the slider can be used as a possibility for calibration of the test fixture.

Change of potential energy when lifting the test specimen and slider is considered as negligible, as displacements are relatively small and the weight of slider and specimen is relatively low. Moreover, uncertainties from measurements of both force and displacement will influence on the results.

Statistical analysis has shown that the polynomial curve fittings and its confidence interval prove that correlation between the analytical solution and the experimental results are existing. A sensitivity analysis of the applied force has shown that a force

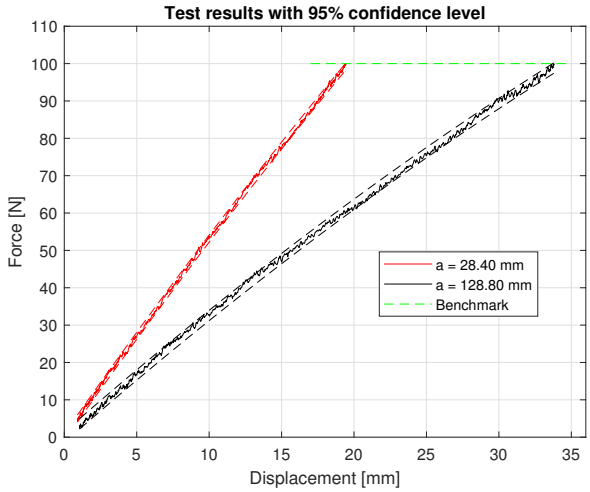

Fig. 2.11: Force-displacement curve for the two different crack lengths. The dashed red and black lines indicates 95 % confidence interval.

equivalent to 102.7 N in the analytical solution would lead to compliance with the experimental result. Therefore, it can be concluded that the validation test with a aluminium alloy specimen and a relative error of 5.6 % is acceptable. Furthermore, other factors and parameters must be studied in order to obtain higher accuracy with this test method. Thereby, it is possible to calibrate the test fixture, and get a higher accuracy of the results.

If tests with Glass Fiber Reinforced Polymer (GFRP) specimens are performed, it is possible to inspect and see the full crack front from above, as this space is free. This gives the opportunity to place a camera and record the crack propagation speed and shape. This kind of inspection can be challenging for other test methods as free space around the test specimen is limited for some test methods.

Future work with the test fixture could be a modification, where it was possible to apply forces in the vertical direction on the test specimen. This would lead to an increase of phase angle, and this will make the TP-MMB more versatile and interesting to use.

2.4 Validation of TP-MMB test method with Cohesive Zone Modeling

Development, design and validation of the TP-MMB test method is performed with Finite Element simulations and use of Cohesive Zone Modeling (CZM). These models are performed in ANSYS software with the formulations this software provides. For the CZM is a bi-linear traction separation law [32] formulation used. This choice of formulation is simple and easy to change in order to get a fast and robust convergence of the non-linear solution. Various traction separation relationships like exponential form [8], constant form [25], polynomial form [67], tri-linear form [97] and linear form [12] are also common used formulations.

A bi-linear traction separation law is illustrated in Figure 2.12, and $\mathrm{K_m}$ is defined as the cohesive layer stiffness and this is often set to be relatively high, as this represent the material behaviour best [74]. However, the rate of robustness and fast convergence depends on maximum traction (σ_m^0), displacement jump at completion of debonding (δ_m^f) and separation at corresponding damage initiation (δ_m^0). If the triangle is relatively flat (isosceles obtuse) it will result in fast convergence and robustness of opposite if the triangle is steep (isosceles acute).

If the cohesive elements are in compression or separation (δ_m) is lower than δ_m^0 the behaviour is linear elastic and damage evolution will not occur. This is shown in Eq. 2.14 where the other intervals also are shown. The damage value (d) is used to degrade $\mathrm{K_m}$ when the separation exceeds δ_m^0. This cohesive layer stiffness can be written as $(1-d)K_m$ in the range between δ_m^0 and δ_m^f. This means that the element will be partially damaged.

The cohesive layer stiffness will remain the same if the new separation does not exceed δ_m^{max}, this is only applicable for common formulation of cohesive elements, as new formulations of cohesive elements are intended for fatigue simulations and the damage value will increase even though the separation is relatively low. These special types of cohesive elements are among others developed and demonstrated by Bak [6] and Turon [96].

$$d = \begin{cases} 0 & \delta_m^0 > \delta_m \\ \frac{\delta_m^f\left(\delta_m - \delta_m^0\right)}{\delta_m\left(\delta_m^f - \delta_m^0\right)} & \delta_m^0 \leq \delta_m < \delta_m^f \\ 1 & \delta_m^f \geq \delta_m \end{cases} \tag{2.14}$$

Griffith's energy approach is still relevant when we use the traction separation law as the integral of the bi-linear function determines the critical energy release rate G_c or fracture energy. This integral is shown in Eq. 2.15 and also illustrated in Figure 2.12.

$$G_c = \int_0^{\delta_m^f} \sigma d\delta \tag{2.15}$$

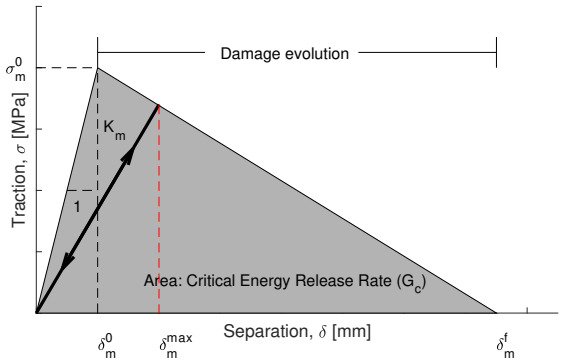

Fig. 2.12: Bi-linear traction-separation law with linear damage evolution. K_m is defined as the cohesive layer stiffness.

As support(B) and support(C) generates two opposite directional forces with the same magnitude, this will result in pure bending moment near the crack tip. This is illustrated in Figure 2.13, where the lower beam is attached to support(A) and the right side is towards support(B) and support(C).

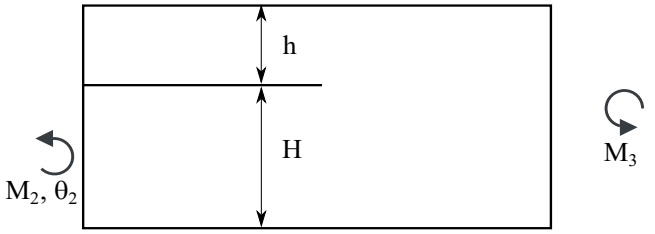

Fig. 2.13: The test specimen is loaded in following way near the crack tip, and the two heights are given as H and h for respectively the lower and upper beam.

These ideal boundary conditions are of cause interrupted by both rolling resistance and gravitational forces. Both effects are eliminated in this simulation in order to demonstrate the new concept.

Different decisions have been made to have a suitable Finite Element model that represent both test fixture functionalities and test specimen behaviour. On the basis

of these decisions, the test specimen is modelled with higher order 3D solid elements. Moreover, the interface between the upper and lower beam is modelled with cohesive elements, as only delamination is studied.

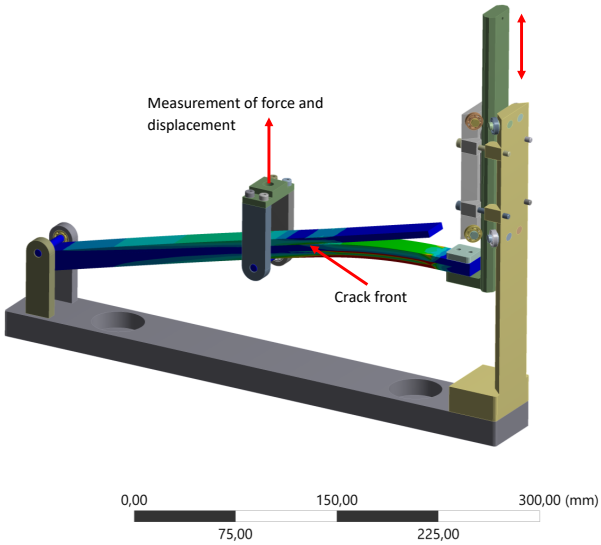

Fig. 2.14: Example of TP-MMB fracture toughness simulation with Cohesive Zone Modeling.

The traction separation law is with a relative low traction in order to have fast convergence and robustness of the solution. The test fixture parts are modelled as rigid bodies, as the stress state in the test fixture is not analyzed in this example. Figure 2.14 illustrates the complete Finite Element model and how test specimen supports and forces are applied. Contact elements, and thereby frictional forces, are not included in this model, as these where unknown.

In the test specimen the fracture process zone is studied as a mix of plane strain and plane stress conditions will appear in the interface between the upper and lower beam. In Figure 2.15 it is seen that the contour bands for shear stresses (τ_{xy}) are super elliptic curved in the fracture process zone as a consequence of mixed plane stress and plane strain conditions. It means that the crack front is ahead in the middle of the test specimen and behind in the sides as was foreseeable and also observed in some of the performed experiments.

The Finite Element simulations showed that the applied forces in support(B) reached a plateau when the fracture process zone was fully developed and steady propagating. This curvature is similar to Figure 2.6 and as the length between support(B) and support(C) is considered constant the bending moment is also constant. Thereby, the

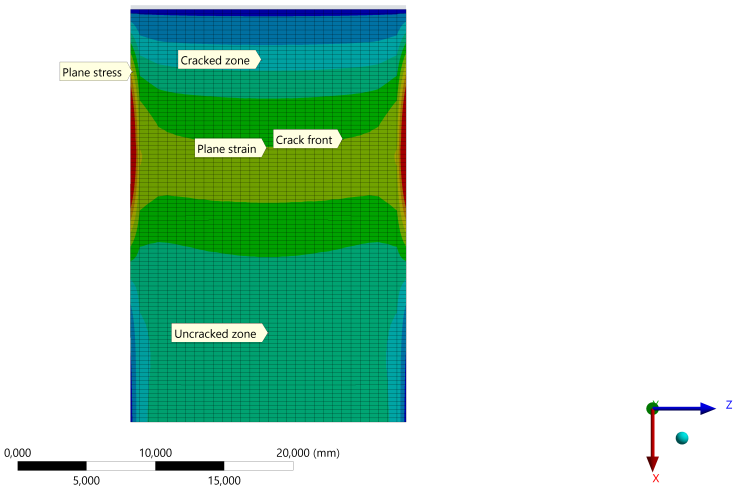

Fig. 2.15: Illustration of the fracture process zone in the interface between the upper and lower beam.

constant bending moment is applied the test specimen and the functionalities of the test fixture fulfills the solution showed in Eq. 2.9. In the design phase of the test fixture several of Finite Element Analysis are performed on components and subcomponents in order to predict the behavior of these components and minimize the amount of used material.

2.5 Fracture toughness testing of uni-directional laminated composite

Delamination tests with relatively high loads are conducted in order to assess performance, limitations and accuracy of both test method and test fixture. Therefore, sixteen test specimens of Unidirectional Directional (UD) GFRP have been produced by Poly-Tech A/S.

These test specimens have a total height (H+h) of 17.90 mm ± 0.15 mm and a width of 20.10 mm ± 0.30 mm. For this reason weight is also examined and the average weight of the test specimens are 272.7 g with a standard deviation of 2.9 g. Moreover, the fracture process zone is placed in the middle of the specimen with a teflon film to initiate the crack front.

The variation of both dimensions and weight will influence on the measured compliance, and it means that these results are held together in order to explain the variation of compliance in a three point bending test. This test is used to approximate the Young's

modulus as this must be assumed consistent.

Figure 2.16 illustrates the normalized mass and normalized stiffness from the preliminary three point bending test of specimens.

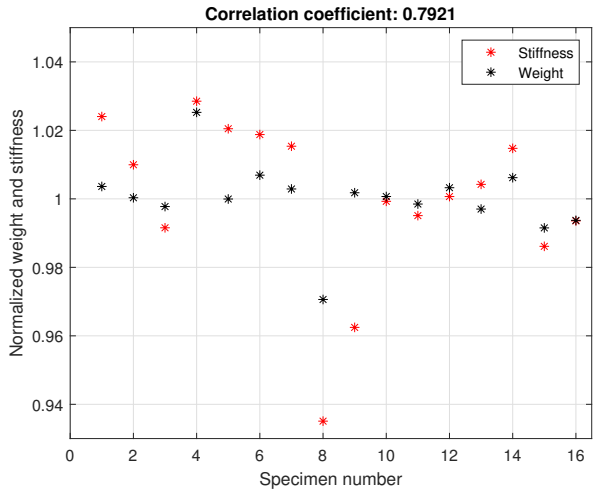

Fig. 2.16: The relatively high correlation coefficient between the normalized stiffness and weight confirms the experimental distribution of stiffness.

It can be concluded that the correlation coefficient is relatively high when the value is 0.7921, and the variation of stiffness primarily can be explained by the deviation of mass and dimensions. It can therefore also be concluded that the density of fibres are sufficiently uniform, and it gave a Young's modulus equivalent to 37,700 MPa, with a standard deviation equivalent to 764 MPa.

Preliminary tests were performed on specimen number 1-11 as these were used for calibration and adjustments of the test fixture in order to obtain stable results. Test specimen 16 was not included in these results as the set up was slightly changed and it would therefore be misleading to include. The presented test was performed on test specimens 12-15, and these results are shown in Figure 2.17. This figure indicates that the applied force starts to be steady when the cross head has moved approximately 32 mm. At this point the applied force is almost 500 N and it starts to be steady around this level as seen in the figure. It means that the fracture resistance is determined with Eq. 2.9 and the fracture toughness is approximately 4.11 mJ/mm^2. This is reasonable and high, as fiber bridging will increase the fracture toughness significantly.

It was observed that a long fracture process zone emerged in the test, and this was due to intensive fiber bridging. This long fracture process zone gave some challenges as the steady state period was relatively short compared to the total period of the test

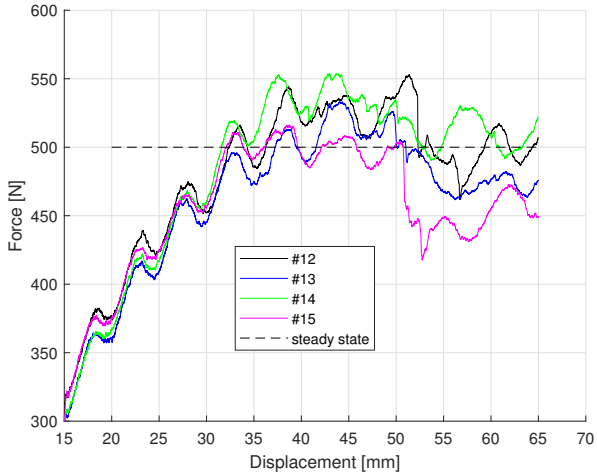

Fig. 2.17: Actual force-displacement curve obtained with test specimen 12-15.

run. The fracture process zone is illustrated in Figure 2.18, and it is easily seen that the fiber bridging is intensive in between the lower and upper beam.

Examination of the slider and roller bearings have shown that high rolling resistance introduces oscillations in the force measurement, and this is easily seen in Figure 2.17. This is caused by the roughness on the surface between the slider and roller bearings.

The test fixture is not intended for fatigue test of laminated composites and adhesive joints, as both roller bearings and slider can be high loaded and these will fail in short time compared to the duration of a typical fatigue test. However, modifications of the test fixture can improve the performance and make the test fixture suitable for fatigue tests.

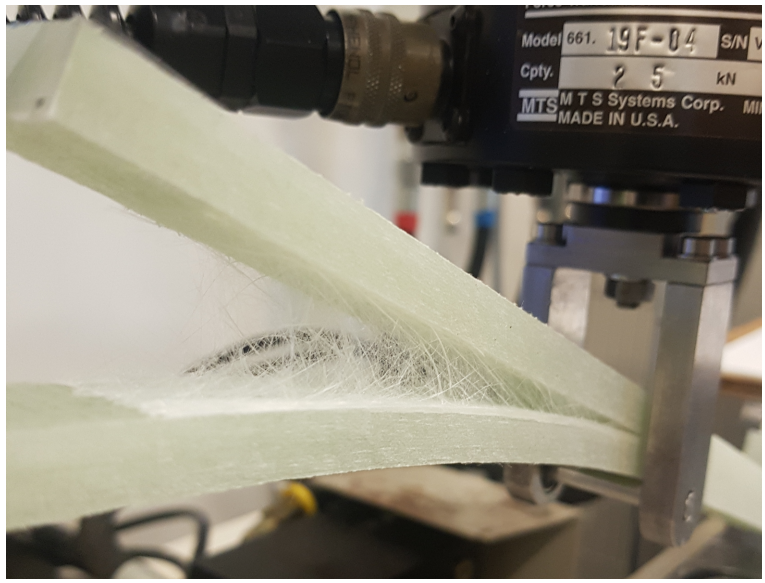

Fig. 2.18: Fiber bridging effect during delamination test in uni-directional laminated composite.

This performance test has shown that the TP-MMB test method has potential for quasi-static fracture resistance testing of laminated composites, and the rolling resistance introduce measurement disturbances when the text fixture is relatively high loaded. Future work could be to modify the test method and apply axial forces to the test specimen in order to increase the phase angle, and have a more versatile test method.

Chapter 3

A linear Finite Element approach to geometric non-linearity

This chapter is based on paper B, C and D, and will be supplemented with additional theory and details. Some of the material in this chapter is adapted with permission from SAGE Journals and Nordic Seminar on Computational Mechanics (NSCM).

3.1 Scientific contribution and impact

This chapter will present three related approaches which all are developed for use in Finite Element Analysis of slender composite structures. All three approaches are providing a novel solution to a known problem which is the computational cost of handling non-linear geometric effects in wind turbine blades. Therefore, the primary contributions of this research is to bring down computational cost and still have high accuracy of the results. These novel solutions will especially be beneficial when fatigue analysis is performed and time is a limiting factor. Moreover, when Finite Element models are getting larger these novel methods be to prefer, as the accuracy can be high and time consumption can be held down.

The presented approaches will also give an improved understanding of the Brazier effect, and thereby give foundations for new simulation methods in this field of research. With the presented methods it is possible to identify the density of the so called Brazier forces in a structure. This possibility will give engineers an opportunity to identify this damaging effect, and with this insight, change design in order to get structural integrity.

3.2 Introduction to the Brazier effect

The Brazier effect [9] has been known for almost 100 years, and is still relevant to take into account when structures are thin-walled and exposed to large deformations. This effect leads to additional forces which can result in inappropriate cross-sectional deformations, that cause high stresses in certain areas of the cross-section. This was studied by Lund and Damkilde [19] in wind turbine blades, and they concluded that especially the stress field in corners of the main spar was relatively high. This can result in crack initiation and propagation over time, which in worst case scenario leads to complete failure of the blade. The problem to failure can be the orientation of fibers, as these are orientated to carry the loads in another direction.

The Brazier effect was also studied by Jensen et. al. [48], and they performed both structural testing and numerical simulations of a 34 m long wind turbine blade in order to predict and identify location of failure caused by contributions from the Brazier effect. Another study [72] with the same blade has also showed that distortion of the cross section is distinct when the blade is exposed to high bending moments and high curvature. This time the blade was exposed to loading both flap and edge wise to investigate certain effects.

Wind turbine blades of today are longer than 110 m, and torsion near the root in these blades are relatively high as deformations are getting larger. This is also a geometric non-linear effect that relate to the Brazier effect, and it was studied in an EUDP-project [47], and different solutions were proposed to address this problem. It was among other things concluded that existing standards were defective regarding the influence of torsional stiffening on eigenfrequencies and fatigue damage.

From other literatures [73] [26] [27] [38] [37] it can also be concluded that geometric non-linearity are contributing to damage in wind turbine blades. Especially the trailing edge is prone to failure caused by contributions from this effect, and the blade segment where the chord length is largest. To understand the Brazier effect this subsection will in details describe the fundamental mechanisms and equations related to this phenomenon. It will give some of the understanding of this effect on how it can be adapted and implemented into Finite Element Analysis.

The original solution derived by Brazier, presents a circular tube that will change to an ellipse in shape, when the cross section is exposed to pure bending. This solution can be adapted to a rectangular tube and the solution is shown in Eq. 3.1 and Eq. 3.2. It gives the explicit relation between crushing pressure (p_c), curvature (κ), bending moment (M), total force in flange (F_σ) Young's modulus (E), distance from center (z) and flange thickness (t_f). The assumption is that $t_f << h$ and the crushing forces in shear webs are inconsiderate. A rectangular thin-walled tube has geometrical similarities with the main spar in a wind turbine blade. Therefore, deformations in this example will be comparable with the behaviour in blades, and Figure 3.1 shows both geometry and parameters for this example.

$$p_c = \frac{\sigma}{R} = \kappa \frac{M}{I} z = \kappa \frac{M}{E\,I} E\,z = \kappa^2\,E\,z \tag{3.1}$$

$$p_c = \frac{\sigma}{R} t_f = \kappa^2\,E\,z\,t_f \tag{3.2}$$

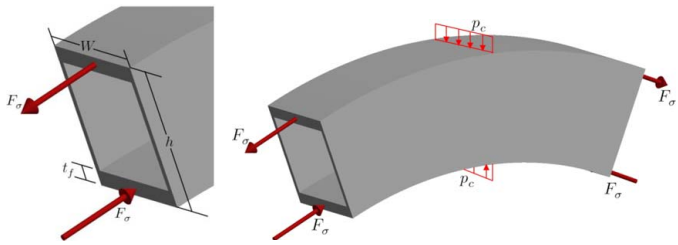

Fig. 3.1: Illustration of thin-walled tube exposed to pure bending moment and crushing pressure.

The crushing pressure will cause inward deformations of the flanges and outward deformations of shear webs as shown in Figure 3.2. It means that area moment of inertia will decrease and differ from the traditional assumption of linear behaviour. However, it is important to mention that buckling will occur in the tube far before maximum of the load carrying capacity is reached. The important part of this effect is not the change of inertia, but instead the additional stress field which cant be ignored.

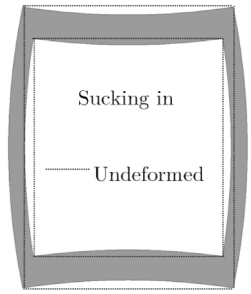

Fig. 3.2: Cross sectional deformation caused by the Brazier effect.

In-plane cross sectional deformations will also appear if a square thin-walled tube is exposed to torsion and deformations are large. This load will results in inward deformation of all four sides as shown in Figure 3.3. The deformations are caused by local

in-plane bending moments in the thin walls as a consequence of large deformations. So the deformation is not caused by an uniform crushing pressure on all four sides, nevertheless the deformations are the same.

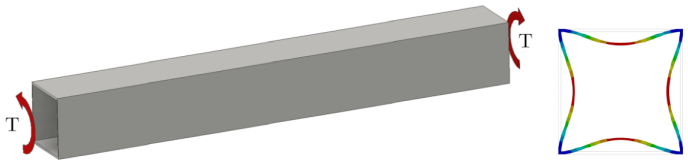

Fig. 3.3: Torsion applied a square thin walled tube and the result is inward deformation of all four sides.

When the tube is exposed to torsion, a reduction of the torsion will constantly appear, and at some point reach a limit. Again, buckling or material strength will be the limiting factor before this maximum is attained. This deformation in combination with shear stresses is causing a linear distribution of the local bending moment in the flanges, where maximum and minimum moment is near the corners. Figure 3.4 shows the distribution of the in-plane bending moment caused by the torsion.

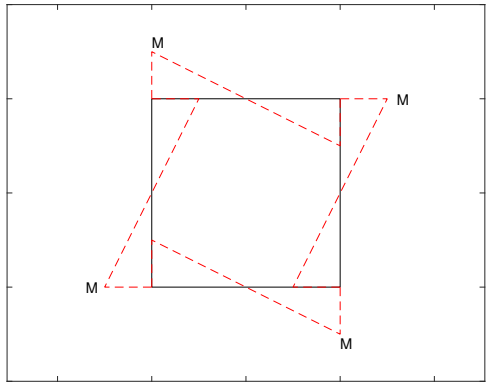

Fig. 3.4: Torsion and large deformation applied a thin walled square tube will result in additional in-plane bending moments.

Zero local bending is in the middle of the flanges in order to have the symmetric deformation, and even small deformations can cause relatively high stresses in the corners of the tube.

This effect is here demonstrated with a numerical solution as an analytical solution for this torsional problem not exists. Therefore, Finite Element Analysis software is used to provide the results for this example. In this example the height to flange thickness ratio $h/t_f = 100$, and the material is isotropic with a Poisson's ratio of 0.3 and a Young's modulus of 200,000 MPa. Moreover, Eq. 3.3 shows the linear relation between angle of twist (θ), torsion (T), length (L), shear modulus (G) and torsion constant (J). This linear assumption is used to find the non-linear relation between torsion constant and in-plane local bending moment.

$$\theta = \frac{T\,L}{G\,J} \tag{3.3}$$

In this example M_{max} is equivalent to the maximum in-plane local bending moment before the sides are in contact with each other, and J_{max} is the torsion constant when the square tube is undeformed. In Figure 3.5 the non-linear relation between local bending moment and torsion constant is illustrated, and it can be concluded from this numerical example that even relatively low bending moment in the flanges will result in a significant drop of the torsion constant.

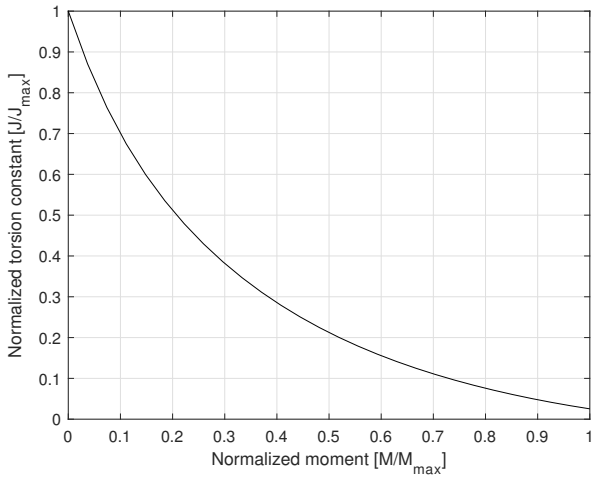

Fig. 3.5: The torsion constant will decrease significant when in-plane local bending moment in the flanges are applied.

These fundamental observations and findings in regular cross sections, are similar to the structural behaviour in wind turbine blades. Especially the structural response from torsion is interesting, as failures caused by this load are relatively new questions in the wind turbine industry that need more attention and understanding. Therefore, if the geometric non-linearity is neglected in evaluation of wind turbine blades, this will have a significant negative impact on the life time performance.

3.3 Large displacements and stress stiffening effects in slender composite structures

Stress stiffening effects in slender blades are pronounced, as axial stiffness is large compared to bending stiffness. This effect gives the coupling between in plane stresses and out of plane stiffness, and when caps, webs and panels are relatively thin this will result in a significant influence on both buckling load and eigenfrequencies of the blade. It means that the orientation of the fibers in the laminates must be considered in combination of these additional loads, as the laminate is not necessarily designed to withstand these stresses.

The Brazier effect and stress stiffening effect are in some extent similar, as the same load case gives the same deformations of a thin walled circular cross section, if the load is much lower than the buckling load.

In Finite Element formulations the stress stiffening effect is defined as the stress stiffness matrix ($\mathbf{K_s}$). This matrix is calculated on a prior solution, as it is a function of stresses, displacements and strains. The solution is shown in Eq. 3.4 and in combination with large rotation and displacements, this will result in a non-linear behaviour that has a major impact on the structural performance and response.

$$\mathbf{K_s} = \int_{(V)} \frac{\partial \mathbf{B}^T(\mathbf{d_0})}{\partial \mathbf{d_0}} \boldsymbol{\sigma} dV \tag{3.4}$$

With the stress stiffness matrix it is possible to find Brazier forces, as these can be considered as external forces instead of internal forces caused by large displacement and the associated stresses. To determine the forces the common direct stiffness method is applied as shown in Eq. 3.5. This gives an approximated displacement vector ($\mathbf{d_0}$), as ($\mathbf{K}$) is the reduced stiffness matrix and ($\mathbf{r_0}$) is the applied external force vector.

$$\mathbf{K}\,\mathbf{d_0} = \mathbf{r_0} \tag{3.5}$$

The prior solution provides opportunity to determine the stress stiffness matrix and in combination with the prior displacement field it is possible to find the additional external forces or Brazier forces ($\mathbf{r_1}$). This operation is shown in Eq. 3.6.

$$\mathbf{K_s}\,\mathbf{d_0} = \mathbf{r_1} \tag{3.6}$$

This results in a new displacement field ($\mathbf{d_1}$) as the Brazier forces are added to the initial external force vector. The reduced stiffness matrix is reused as shown in Eq. 3.7, and the result can be evaluated.

$$\mathbf{K}\,\mathbf{d_1} = \mathbf{r_0} + \mathbf{r_1} \tag{3.7}$$

The additional forces are found by relatively simple mathematical operations, and with this method it is possible to scale the Brazier forces, as we know the Brazier forces are a quadratic function of the applied load to the structure. This is an advantage if this method is used for fatigue analysis of blades as superposition principle can be utilized with these additional forces.

Another way to approximate the additional forces is to perform another type of post processing in each node of the Finite Element model. If nodal forces and displacements in all directions are found, it is possible to find the local rotation and traction force in the nodes if the element is a regular cube. The deformed element will generate additional force components, as the deformations are large. The additional force components are found with few mathematical operations and these can be added to the previous analysis in order to get a better estimate of the stress field caused by the geometric non-linearity.

The calculated force components are primarily pointing towards the center of the main spar in a wind turbine blade if the blade is exposed to flapwise bending. Moreover, the approximated Brazier forces can easily be visualized, and in such a way give insight to the designing engineer, and give foundation to make the best decisions.

3.4 Presentation of the Finite Element based approaches

Linearization of the governing equations in Finite Element formulations is a well known procedure and some examples can be found in following literature [105] [84] [52] [70]. This technique can also be adapted on geometric nonlinearity as we know the stress stiffness matrix is inconsistent in a structural analysis. Therefore, this section will describe and demonstrate three linearizations to this problem, and how accurate these perform.

Three types of linear approaches to handle geometric non-linearity for Finite Element Analysis are established. The first approach is able to handle the geometric effects associated with bending, and the second approach is able to find the additional forces, that occur when a thin-walled cross section is exposed to torsion. Last approach is able to handle all types of load cases and the results are still of high accuracy.

All three approaches are based on a two step procedure that requires post processing of the first solution in order to determine the additional forces and apply these to the second step. The Finite Element Analysis are performed with ANSYS software, and the post processing procedures and calculations are performed with MATLAB software. Output of these calculations are the additional forces which are combined with the prior model and a new solution is found, as shown in Figure 3.6.

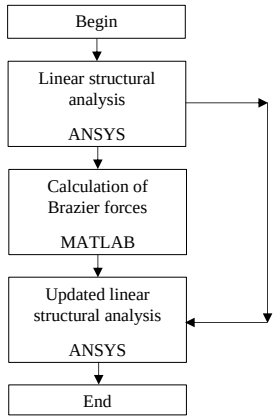

Fig. 3.6: Flow chart of Finite Element approach procedure.

The first approach calculates Brazier forces perpendicular to the beam axis caused by bending, and the calculations are performed individually for each node in the element. In this example is an eight node element used. It means that nodal stresses, position and deformations are retrieved from the first linear structural analysis in order to have these data for the novel algorithm.

Figure 3.7 shows the parameters needed in order to perform the calculations showed in Eq. 3.8 and Eq. 3.9. With some of these data it is possible to calculate the two areas ($A_{n,xy}$) of the element perpendicular to the beam axis. Only if the elements are regular, and all sides are general orientated according to a Cartesian coordinate system, will the developed algorithm perform with precise results. From nodal positioning and deformation it is possible to approximate two planes and find the change of angle ($\Delta\theta$) between these in both x and y direction. It defines the direction of the Brazier force in combination with the sign of the axial average stress ($\overline{\sigma}_{zz}$).

$$F_{x,Brazier} = \frac{A_{1,xy} + A_{2,xy}}{2} \sin\left(\Delta\theta_{u,w}\right) \frac{1}{8} \sum_{n=1}^{8} \sigma_{n,zz} \tag{3.8}$$

$$F_{y,Brazier} = \frac{A_{1,xy} + A_{2,xy}}{2} \sin\left(\Delta\theta_{v,w}\right) \frac{1}{8} \sum_{n=1}^{8} \sigma_{n,zz} \tag{3.9}$$

Average area and axial stresses multiplied obviously give the axial force acting on the element, and the change of angle also defines the magnitude of the Brazier force component ($F_{x,Brazier}, F_{y,Brazier}$). This force can be treated as a volumetric load acting on the element, and this force is equally divided and distributed into all nodes of the element.

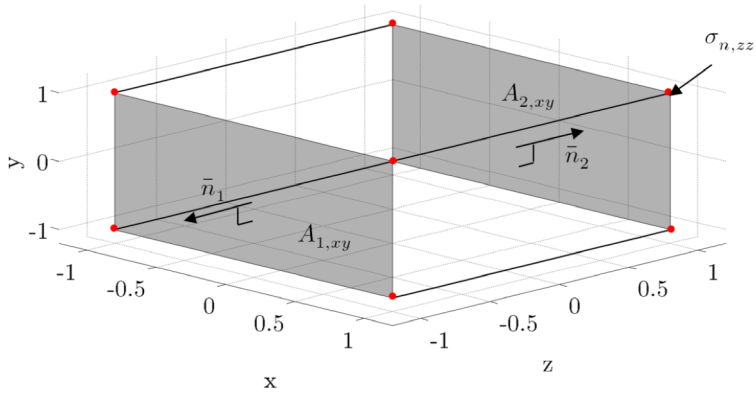

Fig. 3.7: Parameters retrieved and calculated for each element.

When these forces are calculated and assembled with the neighboring elements, these can be applied to the first structural analysis. This will give an updated external force vector which can describe the geometric non-linearity. It is an advantage to visualise the new force vector in the numerical model as it confirms the distribution of contributing forces in the structure. This is easily seen in Figure 3.8 where the magnitude of the forces as expected are high in the load carrying main spar. Furthermore, it is important to notice the horizontal forces in the top and bottom cap as these forces are pointing in opposite directions and this will lead to so called shear distortion [49] of the cross section, which can be damaging for the blade.

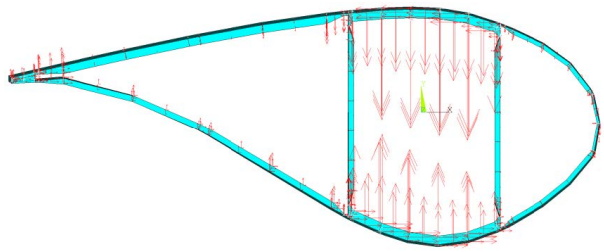

Fig. 3.8: Visualization of Brazier forces acting on a cross section at a specific distance from the root. The wind turbine blade is primarily exposed to flapwise bending.

Another advantage with this method is the possibility of scaling forces with a quadratic function for a fatigue analysis of the composite structures. This will give computational savings depending on the degree of geometric non-linearity.

Second approach addresses the problem regarding geometric non-linearity due to torsion in thin-walled cross sections. This approach is an expansion of the torsion idea explained in Chapter 3.2. as this approach is able to handle other types of uniform cross sections and the accuracy of the approximated stress field is still high. An example is shown in Figure 3.9. The calculations are different in the second approach, as deformation caused by torsion will result in an offset of the two gray planes showed in Figure 3.7. The planes are still parallel, but this offset in combination with shear stresses will result in a local bending moment. This local bending moment is calculated and applied to the updated model.

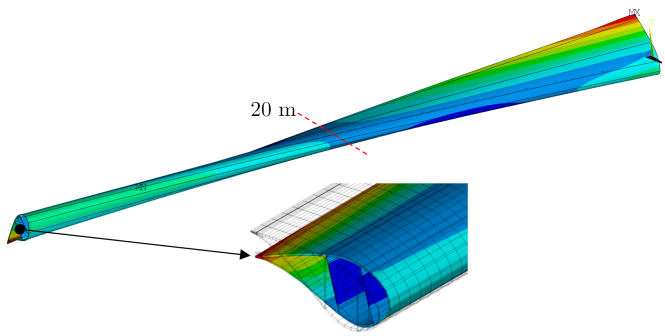

Fig. 3.9: Uniform cross section applied pure torsion where center is analyzed for geometric non-linearity.

Approximations from the second linear approach has shown that contributing forces or significant change of geometric stiffness are concentrated near the trailing edge as seen in Figure 3.10. Moreover, the corners between the spar cap and shear webs also

seem to be relatively high loaded.

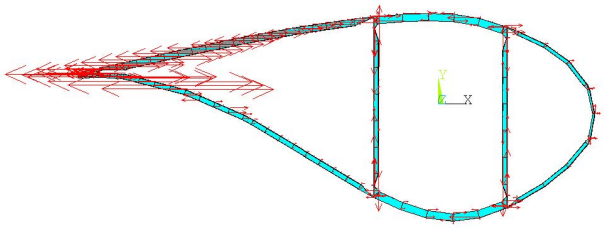

Fig. 3.10: The linear approach shows that contributing forces primarily are concentrated near the trailing edge.

The non-linear solution is assumed to give the correct results and both the linear analysis and the linear approach is compared with this non-linear solution in order to evaluate the performance of these. In Figure 3.11 it is seen that the panels between the main spar and the trailing edge are moving inwards if the blade is only exposed to torsion. The linear solution is not capable of capturing anything of this effect as foreseen. However, the linear approach is almost identical to the non-linear solution, and this will result in a good approximation of the associated stress field.

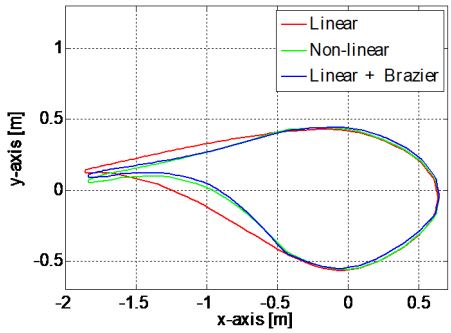

Fig. 3.11: Results from the three methods give different response of deformations and the non-linear analysis is considered as the correct output. Deformation scale factor: 40.

It can be concluded that second approach performs with very high accuracy in this example. It can also be concluded that torsion can lead to failure in the trailing edge, as local deformations are relatively high, which can lead to stress levels that exceed material strength and fracture resistance.

Third approach is able to handle all types of load cases, and determine the associated contributing forces. This approach apply the advantages of the stress stiffness matrix,

which is the key to find these forces. So, changing and updating the external force vector with this approach will give the structural behaviour caused by geometric non-linearity. Fundamentals and details regarding this method are described in Chapter 3.3, and here demonstrated in a Finite Element Analysis of a 34 m long wind turbine blade.

The 34 m long blade is exposed to a three point combined loading both flapwise and edgewise. The combined load case will lead to distinct geometric non-linearity and the segment 4 m to 12 m is therefore primarily analysed as bending moments are high in this segment. The high bending moments will lead to local cross sectional deformations and significant change of the stress field. This will give some challenges as a linear analysis will not be able to capture this structural behaviour.

Figure 3.12 shows an illustrative comparison of the linear and non-linear stress field. It illustrates the absolute error with a threshold of 2 MPa, and the gray areas indicate an error larger than 2 MPa. On the panels it is easily seen that error is comprehensive, and also in trailing edge and on the caps these large deviations are seen. It can be concluded that the linear solution differ significantly from the non-linear solution and this gives an inappropriate approximation of the stress field.

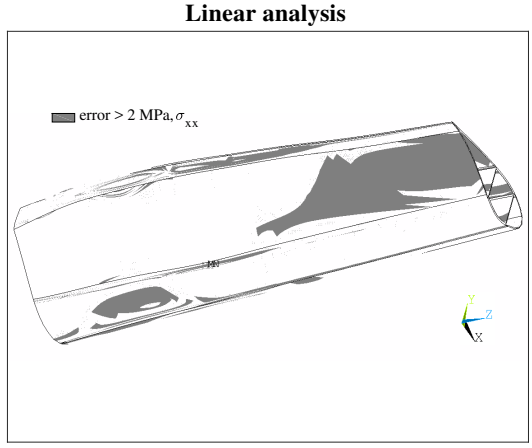

Fig. 3.12: The figure shows the wind turbine blade in a range of 4 m to 12 m, and the gray areas indicate an absolute error larger than 2 MPa for in-plane stresses (σ_{xx}) compared to the non-linear solution.

The presented approach improves the accuracy of the stress field, and this is seen in Figure 3.13 where the gray areas are reduced. This solution differ slightly on the pressure side panel as the circular gray contours are relatively small, compared to the linear solution. An absolute error larger than 2 MPa are found elsewhere in the blade, and these errors are considered acceptable as these areas are relatively small.

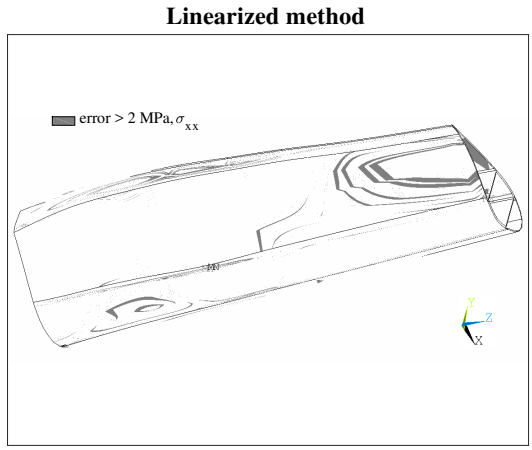

Fig. 3.13: The figure shows the wind turbine blade in a range of 4 m to 12 m, and the gray areas indicate an absolute error larger than 2 MPa for in-plane stresses (σ_{xx}) compared to the non-linear solution.

Analysing in-plane bending stresses (σ_{xx}) in all nodes, has shown that the linear approach improves the solution markedly, as the relative error is reduced. The relative error is based on the non-linear solution which can be seen in Figure 3.14, where a histogram illustrates the distribution of the relative error for respectively a linear solution and the presented approach. In the range of 0% to 90% 28,340 nodes are presented from the linear solution and 33,527 nodes from the novel approach. In total 43,592 nodes are analyzed and the rest of these results has a relative error larger than 90%.

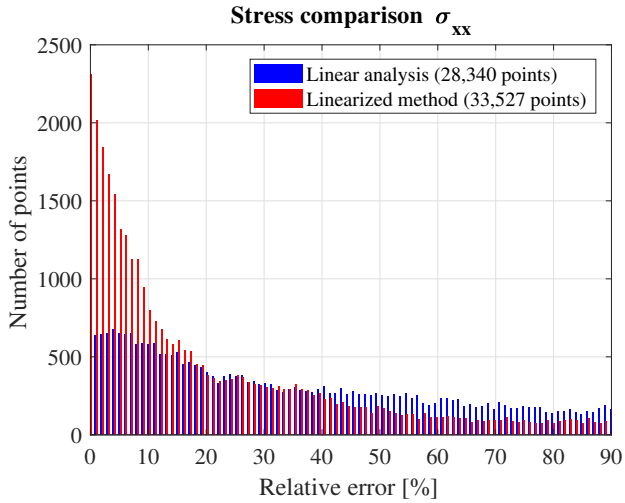

Fig. 3.14: Histogram of relative error for different types of analysis.

An extensive difference is seen in the range 0 - 0.5 %, as 649 and 2,310 results are presented for the two types of analysis. This is almost a factor of four and it is clear that the novel approach comes up with results closer to the correct answer, as the results are more concentrated near zero. The relative error for the novel approach is almost exponentially distributed and the linear analysis possesses a linear decay of error.

It can be concluded that all three presented approaches have different advantages and disadvantages. Each approach is suitable for different load cases and the accuracy depends on many parameters. However, with a little extra of computational effort, the accuracy of the approximated stress field will be improved noticeable.

The two first approaches are not tested against the last method, as these methods are designed for a specific purpose and regular geometries with a regular Finite Element mesh.

So finally this chapter has described and demonstrated that the presented approaches have potential for structural analysis of wind turbine blades. These approaches are especially suitable for fatigue analysis, and will come up with significant better approximations of the stress field than linear analysis.

Chapter 4

Discussion and concluding remarks

This research is based on an increasing demand from the wind turbine blade industry to test and simulate the structural behaviour of laminated composites. Composite materials are pushed to the limit of strength and fatigue resistance, in order to reduce weight, find economic savings and have reduction in cost of wind power.

This optimization process results in longer and more slender blades, and this increase of length entails new challenges like e.g. geometric non-linearity. From the literature review it can be concluded that geometric non-linearity is of special interest, as it can lead to crack propagation in the trailing edge. Moreover, from the literature review it can also be concluded that fracture mechanics and fatigue in structures are fields of research which are far from depleted, as accidents still are to come caused by these phenomenons.

Modern wind turbine blades are high level engineering, and it requires new test methods and simulation tools in order to ensure structural integrity. Moreover, new methods will help understanding the nature of fatigue and fracture mechanics in composite structures, and thereby ensure high lifetime performance. On the basis of these specific challenges this research has contributed with both a novel structural test method (TP-MMB) and Finite Element analysing algorithms for thin walled composite structures.

The main contributions of this PhD project are:

- A novel test fixture and test method (TP-MMB) which are able to determine fracture resistance in both laminated composites, bi-materials and adhesive joints. This method is also able to handle fiber bridging and it requires a minimum of measuring equipment. (Paper A)
- A Finite Element approach which is capable of converting the change of geometric stiffness into external forces. This approach can handle all types of load cases with relative low computational cost and high accuracy. (Paper B)
- A Finite Element approach which is capable to determine Brazier forces in regular thin walled geometries exposed to pure bending. (Paper C and D)
- A Finite Element approach which is capable to determine Brazier forces in regular thin walled geometries exposed to torsion. (Paper C and D)

We start with the novel test apparatus which has been designed for determination of cohesive strength in laminated composites, adhesive joints and bi-material interfaces. This invention will give a scientific impact, as an analogous test apparatus has not been found in literature, and similarities are only found in the governing equations used for determination of fracture resistance. Moreover, this test method can easily fit into a standard tensile testing machine and it is capable of finding fracture toughness for a phase angle equivalent to 41°. It can also be concluded that many other test methods are designed for either fracture mode I or fracture mode II, and only a few methods are versatile and able to handle mode mixity like this method. A Finite Element Analysis of a quasi static fracture toughness test has also proved the potential in TP-MMB test method. This prior work, investigations and simulations gave the basis to manufacture and perform a validation test. The validation test was performed with an aluminium alloy bar in order to have a controlled crack front and have a homogeneous material with linear behaviour of elasticity. These results were successful, and minor problems was found regarding rolling resistance between slider and roller bearings when applied loads were high. Future work will be to reduce and compensate for rolling resistance between slider and roller bearings in order to have results with higher accuracy.

It can also be concluded that the TP-MMB test method is able to handle twice as long test specimens than a four point bending test fixture, if the test fixture must fit into a standard tensile testing machine. This advantage is preferable if large scale fiber bridging occur, as it will give a longer period of stable crack propagation with the presented method. Another advantage with the TP-MMB is the opportunity to measure the variation of measured forces caused by only one crack front instead of two in a four point bending test.

This research has also proved that the TP-MMB test method has potential for fatigue testing of laminated composites and adhesive joints. However, it requires modification

of the slider system, which must be more robust and have lower rolling resistance. These modifications will result in better approximations of crack growth rate and the associated stress intensity factor.

Future work with the TP-MMB test method is to compare it with other test methods which is capable of generating a mode mixity with a phase angle equivalent to 41°, and find possible deviations. These studies will enhance the novel solution and underline the possibilities with this test method.

Chapter 3 covers the three Finite Element approaches which in a new way can approximate Brazier forces and the associated stress field caused by large deformation and rotation in thin walled composite structures. These approaches are primarily intended for fatigue analysis of wind turbine blades, as these analysis are time consuming and require high computational effort if geometric non-linearity is included. Furthermore, from the literature review it can be concluded that geometric non-linearity is an increasing problem causing new failure modes in the blades, as these are getting longer and more slender. Therefore, rational simulation methods are needed, in order to save time and get acceptable approximations of the stress field. Thereby, these approaches will have a scientific impact, as these in a new way can account for geometric non-linearity.

The first Finite Element approach is based on the classic phenomenon presented by Brazier in 1927, where pure bending is applied a regular geometry. This approach is reformulated and an algorithm is developed for Finite Element use. It can be concluded that this algorithm perform with high accuracy and it can bring down computational time. It can also be concluded that this approach can easily be implemented into commercial Finite Element software.

From the literature review it can also be concluded that torsion in blades is an increasing problem as these are getting longer and more slender. This trend leads to new failure modes in the blades, and these can appear in the trailing edge. Therefore, an algorithm to handle this effect was developed for uniform cross sections. This algorithm is also performing with high accuracy, and a study with an uniform wind turbine blade cross section confirmed this. Both deformations and stress field were almost identical with the non-linear solution in this example, and it means that the understanding of this torsion effect in blades is correct understood and applied.

The last numerical approach is intended for general use in 3D Finite Element Analysis where geometric non-linearity has a significant impact on change of the stress field. This method uses the information kept in the stress stiffness matrix and convert it into external forces. It entails that time consuming matrix factorization is avoided, and computational time is held down. In Paper B it was demonstrated that this method performs with relatively high accuracy.

From this research it can also be concluded, that all three approaches allow for scaling of the calculated forces, and the approximated outcome is acceptable. On the basis of the present work, it can also be concluded that all three Finite Element approaches have large potential in forthcoming simulation tools for slender composite structures.

In general this PhD project has contributed with methods which can improve current design methods for wind turbine blades. Furthermore, it will improve structural testing and understanding of where and how to use composite materials in wind turbine blades, and this research thereby answers the scientific question raised in this project.

References

[1] "ASTM D6671 / D6671M - Standard Test Method for Mixed Mode I-Mode II Interlaminar Fracture Toughness of Unidirectional Fiber Reinforced Polymer Matrix Composites." [Online]. Available: https://www.astm.org/Standards/D6671.htm

[2] A. Wöhler, "Versuche zur Ermittlung der auf die Eisenbahnwagenachsen einwirkenden Kräfte und die Widerstandsfähigkeit der Wagen-Achsen," *Zeitschrift für Bauwesen*, vol. X, pp. 583–616, 1860.

[3] W. A. J. Albert, *Über Treibseile am Harz, Archive für Mineralogie Geognosie Bergbau und Hüttenkunde, vol. 10, pp 215-34*, 1838.

[4] M. E. Asl, C. Niezrecki, J. Sherwood, and P. Avitabile, "Similitude analysis of composite i-beams with application to subcomponent testing of wind turbine blades," in *Experimental and Applied Mechanics, Volume 4*, C. Sciammarella, J. Considine, and P. Gloeckner, Eds. Cham: Springer International Publishing, 2016, pp. 115–126.

[5] ——, "Scaled Composite I-Beams for Subcomponent Testing of Wind Turbine Blades: An Experimental Study," in *Mechanics of Composite and Multi-functional Materials, Volume 6*, P. R. Thakre, R. Singh, and G. Slipher, Eds. Cham: Springer International Publishing, 2018, pp. 71–78.

[6] B. L. Bak, A. Turon, E. Lindgaard, and E. Lund, "A benchmark study of simulation methods for high-cycle fatigue-driven delamination based on cohesive zone models," *Composite Structures*, vol. 164, pp. 198–206, mar 2017.

[7] B. L. V. Bak, A. Turon, E. Lindgaard, and E. Lund, "A simulation method for high-cycle fatigue-driven delamination using a cohesive zone model," *International Journal for Numerical Methods in Engineering*, vol. 106, no. 3, pp. 163–191, 2016. [Online]. Available: https://onlinelibrary.wiley.com/doi/abs/10.1002/nme.5117

[8] G. Barenblatt, "The mathematical theory of equilibrium cracks in brittle fracture," ser. Advances in Applied Mechanics, H. Dryden, T. von Kàrmàn, G. Kuerti, F. van den Dungen, and L. Howarth, Eds. Elsevier, 1962, vol. 7, pp. 55 – 129. [Online]. Available: http://www.sciencedirect.com/science/article/pii/S0065215608701212

[9] L. G. Brazier, "On the Flexure of Thin Cylindrical Shells and Other "Thin" Sections," *Proceedings of the Royal Society A: Mathematical, Physical and Engineering Sciences*, vol. 116, no. 773, pp. 104–114, sep 1927. [Online]. Available: http://rspa.royalsocietypublishing.org/cgi/doi/10.1098/rspa.1927.0125

[10] W. Brocks, *Plasticity and Fracture*, ser. Solid Mechanics and Its Applications. Cham: Springer International Publishing, 2018, vol. 244. [Online]. Available: http://link.springer.com/10.1007/978-3-319-62752-6

[11] A. J. Brunner, N. Murphy, and G. Pinter, "Development of a standardized procedure for the characterization of interlaminar delamination propagation in advanced composites under fatigue mode I loading conditions," 2009. [Online]. Available: https://ac.els-cdn.com/S0013794409002392/1-s2.0-S0013794409002392-main.pdf?{_}tid=32375132-c1f4-437c-ba48-5460a969d221{&}acdnat=1521035849{_}a012dda985b2752d8332d35b6c235614

[12] G. Camacho and M. Ortiz, "Computational modelling of impact damage in brittle materials," *International journal of solids and structures*, vol. 33, no. 20-22, pp. 2899–2938, 1996.

[13] L. Carreras, J. Renart, A. Turon, J. Costa, B. L. Bak, E. Lindgaard, F. Martin de la Escalera, and Y. Essa, "A benchmark test for validating 3D simulation methods for delamination growth under quasi-static and fatigue loading," *Composite Structures*, vol. 210, pp. 932–941, feb 2019.

[14] P. G. Charalambides, H. C. Cao, J. Lund, and A. G. Evans, "Development of a test method for measuring the mixed mode fracture resistance of bimaterial interfaces," *Mechanics of Materials*, vol. 8, no. 4, pp. 269–283, 1990.

[15] G. P. Cherepanov, "Crack propagation in continuous media. PMM vol. 31, no. 3, 1967, pp. 476-488," *Journal of Applied Mathematics and Mechanics*, vol. 31, no. 3, pp. 503–512, 1967.

[16] D. I. Chortis, *Nonlinear Dynamic Response of Composite Plate-Beams*. Heidelberg: Springer International Publishing, 2013, pp. 103–150. [Online]. Available: https://doi.org/10.1007/978-3-319-00864-6_5

[17] N. Clark, "New Cracks Found in Wings of Airbus A380 Planes - New York Times," 2012, https://www.nytimes.com/2012/01/20/business/global/a380-jets-may-get-closer-inspections.html, last accessed on 19/08/19.

[18] J. J. Connor and S. Faraji, *Introduction to Structural Engineering*. Cham: Springer International Publishing, 2016, pp. 3–45. [Online]. Available: https://doi.org/10.1007/978-3-319-24331-3_1

[19] L. Damkilde and B. Lund, "A simplified analysis of the brazier effect in composite beams." Chalmers tekniska högskola, 2007, null ; Conference date: 23-11-2007 Through 24-11-2007.

[20] P. Davies, B. R. K. Blackman, and A. J. Brunner, "Standard Test Methods for Delamination Resistance of Composite Materials: Current Status," *Applied Composite Materials*, vol. 5, no. 6, pp. 345–364, 1998. [Online]. Available: http://link.springer.com/10.1023/A:1008869811626

[21] P. Davies, G. D. Sims, B. R. Blackman, A. J. Brunner, K. Kageyama, M. Hojo, K. Tanaka, G. Murri, C. Rousseau, B. Gieseke, and R. H. Martin, "Comparison of test configurations for determination of mode II interlaminar fracture toughness results from international collaborative test programme," *Plastics, Rubber and Composites Processing and Applications*, vol. 28, no. 9, pp. 432–437, 1999. [Online]. Available: https://www.tandfonline.com/doi/abs/10.1179/146580199101540600

[22] R. Dekker, F. van der Meer, J. Maljaars, and L. Sluys, "A cohesive xfem model for simulating fatigue crack growth under mixed-mode loading and overloading," *International Journal for Numerical Methods in Engineering*, vol. 118, no. 10, pp. 561–577, 2019. [Online]. Available: https://onlinelibrary.wiley.com/doi/abs/10.1002/nme.6026

[23] " DNVGL-ST-0376, Rotor blades for wind turbines," Det Norske Veritas - Germanischer Lloyd, Standard, Dec. 2015.

[24] C. W. Dolan and H. R. T. Hamilton, *Basic Concepts, Prestressed Concrete: Building, Design, and Construction*. Cham: Springer International Publishing, 2019, pp. 1–30. [Online]. Available: https://doi.org/10.1007/978-3-319-97882-6_1

[25] D. Dugdale, "Yielding of steel sheets containing slits," *Journal of the Mechanics and Physics of Solids*, vol. 8, no. 2, pp. 100 – 104, 1960. [Online]. Available: http://www.sciencedirect.com/science/article/pii/0022509660900132

[26] M. Eder and R. Bitsche, "A qualitative analytical investigation of geometrically nonlinear effects in wind turbine blade cross sections," *Thin-Walled Structures*, vol. 93, pp. 1 – 9, 2015. [Online]. Available: http://www.sciencedirect.com/science/article/pii/S0263823115000798

[27] M. Eder, R. Bitsche, and F. Belloni, "Effects of geometric non-linearity on energy release rates in a realistic wind turbine blade cross section," *Composite Structures*, vol. 132, pp. 1075–1084, 07 2015.

[28] A. Evans and J. Hutchinson, "Effects of non-planarity on the mixed mode fracture resistance of bimaterial interfaces," *Acta Metallurgica*, vol. 37, no. 3, pp. 909 – 916, 1989. [Online]. Available: http://www.sciencedirect.com/science/article/pii/0001616089900175

[29] M. Eydani Asl, C. Niezrecki, J. Sherwood, and P. Avitabile, "Predicting the vibration response in subcomponent testing of wind turbine blades," in *Special Topics in Structural Dynamics, Volume 6*, R. Allemang, Ed. Cham: Springer International Publishing, 2015, pp. 115–123.

[30] L. Ferry, D. Perreux, D. Varchon, and N. Sicot, "Fatigue behaviour of composite bars subjected to bending and torsion," *Composites Science and Technology*, vol. 59, no. 4, pp. 575 – 582, 1999. [Online]. Available: http://www.sciencedirect.com/science/article/pii/S0266353898001031

[31] A. C. Fischer-Cripps, *Introduction to Contact Mechanics*, ser. Mechanical Engineering Series. Boston, M. A.: Springer US, 2007. [Online]. Available: http://link.springer.com/10.1007/978-0-387-68188-7

[32] P. H. Geubelle and J. S. Baylor, "Impact-induced delamination of composites: a 2d simulation," *Composites. Part B, Engineering*, vol. 29, no. 5, pp. 589–602, 1998.

[33] A. A. Griffith, "The Phenomena of Rupture and Flow in Solids," *Philosophical Transactions of the Royal Society A: Mathematical, Physical and Engineering Sciences*, vol. 221, no. 582-593, pp. 163–198, jan 1921. [Online]. Available: http://rsta.royalsocietypublishing.org/cgi/doi/10.1098/rsta.1921.0006

[34] M. E. Gurtin, "The Linear Theory of Elasticity," in *Linear Theories of Elasticity and Thermoelasticity*. Berlin, Heidelberg: Springer Berlin Heidelberg, 1973, pp. 1–295. [Online]. Available: http://link.springer.com/10.1007/978-3-662-39776-3{_}1

[35] B. Harris, N. Gathercole, H. Reiter, and T. Adam, "Fatigue of carbon-fibre-reinforced plastics under block-loading conditions," *Composites Part A: Applied Science and Manufacturing*, vol. 28, no. 4, pp. 327 – 337, 1997. [Online]. Available: http://www.sciencedirect.com/science/article/pii/S1359835X96001315

[36] M. D. Harris, W. J. Grogg, A. Akoma, B. J. Hayes, R. F. Reidy, E. F. Imhoff, and P. C. Collins, "Revisiting (Some of) the Lasting Impacts of the Liberty Ships via a Metallurgical Analysis of Rivets from the SS âœJohn W. Brownâ," *JOM*, vol. 67, no. 12, pp. 2965–2975, dec 2015. [Online]. Available: http://link.springer.com/10.1007/s11837-015-1668-1

[37] P. Haselbach, M. Eder, and F. Belloni, "A comprehensive investigation of trailing edge damage in a wind turbine rotor blade," *Wind Energy*, vol. 19, pp. n/a–n/a, 10 2016.

[38] P. U. Haselbach and K. Branner, "Initiation of trailing edge failure in full-scale wind turbine blade test," *Engineering Fracture Mechanics*, vol. 162, pp. 136 – 154, 2016. [Online]. Available: http://www.sciencedirect.com/science/article/pii/S0013794416302065

[39] P. Haselbach, R. Bitsche, and K. Branner, "The effect of delaminations on local buckling in wind turbine blades," *Renewable Energy*, vol. 85, pp. 295–305, jan 2016. [Online]. Available: http://linkinghub.elsevier.com/retrieve/pii/S0960148115300756

[40] K. Holm-Jørgensen, J. Larsen, and S. Nielsen, "On the nonlinear structural analysis of wind turbine blades using reduced degree-of-freedom models," *Structural Engineering and Mechanics*, vol. 28, no. 1, pp. 107–127, 2008.

[41] J. W. Hutchinson and Z. Suo, "Mixed Mode Cracking in Layered Materials," *Advances in Applied Mechanics*, vol. 29, no. C, pp. 63–191, jan 1991.

[42] " IEC 61400-23:2014 - Wind turbines - Part 23: Full-scale structural testing of rotor blades," International Electrotechnical Commission, Standard, Apr. 2014.

[43] K.-H. Im, C.-S. Cha, S.-K. Kim, and I.-Y. Yang, "Effects of temperature on impact damages in CFRP composite laminates," *Composites. Part B, Engineering*, vol. 32, no. 8, pp. 669–682, 2001.

[44] C. E. Inglis, "Stresses in a plate due to the presence of cracks and sharp corners," pp. 3–17, 1913. [Online]. Available: https://www.scirp.org/(S(351jmbntvnsjt1aadkposzje))/reference/ReferencesPapers.aspx?ReferenceID=680158

[45] G. R. Irwin, "Fracture," 1958, pp. 551–590. [Online]. Available: http://link.springer.com/10.1007/978-3-642-45887-3{_}5

[46] F. M. Jensen, *Ultimate Strength of a large wind turbine blade.* LAP Lambert Academic Publishing, 2010.

[47] ——, *EUDP-LEX Project Technical description, Project 64013-0115.* Bladena, 2013-2016.

[48] F. Jensen, B. Falzon, J. Ankersen, and H. Stang, "Structural testing and numerical simulation of a 34m composite wind turbine blade," *Composite Structures*, vol. 76, no. 1-2, pp. 52–61, 2006.

[49] F. Jensen, P. Weaver, L. Cecchini, H. Stang, and R. Nielsen, "The brazier effect in wind turbine blades and its influence on design," *Wind Energy*, vol. 15, no. 2, pp. 319–333, 2012.

[50] J. B. Jørgensen, B. F. Sørensen, and C. Kildegaard, "Adhesive Joints in Wind Turbine Blades," 2017. [Online]. Available: http://orbit.dtu.dk/en/publications/adhesive-joints-in-wind-turbine-blades(350b2a9b-9246-45dc-a496-6ae99c8749f5).html

[51] A. R. Khoei, *Extended Finite Element Method.* Chichester, UK: John Wiley & Sons, Ltd, dec 2014. [Online]. Available: http://doi.wiley.com/10.1002/9781118869673

[52] N.-H. Kim, *Finite Element Analysis for Nonlinear Elastic Systems.* New York, NY: Springer US, 2015, pp. 141–239. [Online]. Available: https://doi.org/10.1007/978-1-4419-1746-1_3

[53] S. Laustsen, E. Lund, L. Kühlmeier, and O. Thomsen, "Failure behaviour of grid-scored foam cored composite sandwich panels for wind turbine blades subjected to realistic multiaxial loading conditions," *Journal of Sandwich Structures Materials*, vol. 16, no. 5, pp. 481–510, 2014.

[54] ——, "High-fidelity multiaxial testing of composite substructures," in *16th European Conference on Composite Materials, ECCM 2014.* European Conference on Composite Materials, ECCM, 2014, null ; Conference date: 22-06-2014 Through 26-06-2014.

[55] E. Lindgaard, B. Bak, J. Glud, J. Sjølund, and E. Christensen, "A user programmed cohesive zone finite element for ansys mechanical," *Engineering Fracture Mechanics*, vol. 180, pp. 229–239, Jul. 2017.

[56] H. Lovell. (2019) Air Force grounds more than 100 of C-130 aircraft after atypical cracking discovered. https://www.washingtonexaminer.com/news/air-force-grounds-more-than-100-of-c-130-aircraft-after-atypical-cracking-discovered, last accessed on 19/08/19.

[57] E. Lund and J. Sjølund, "On gradient based structural optimization of a wind turbine blade," in *Proceedings of 21st International Conference on Composite Materials*. International Committee on Composite Materials, 2017, null ; Conference date: 20-08-2017 Through 25-08-2017. [Online]. Available: http://www.iccm21.org/

[58] J. Machado, E. Marques, R. Campilho, and L. F. da Silva, "Mode I fracture toughness of CFRP as a function of temperature and strain rate," *Journal of Composite Materials*, vol. 51, no. 23, pp. 3315–3326, sep 2017. [Online]. Available: http://journals.sagepub.com/doi/10.1177/0021998316682309

[59] G. Marsh, "The challenge of wind turbine blade repair - Renewable Energy Focus," 2011, http://www.renewableenergyfocus.com/view/21860/the-challenge-of-wind-turbine-blade-repair/, last accessed on 09/08/19.

[60] G. Martakos, J. H. Andreasen, C. Berggreen, and O. T. Thomsen, "Interfacial crack arrest in sandwich beams subjected to fatigue loading using a novel crack arresting device - Numerical modelling," *Journal of Sandwich Structures and Materials*, vol. 21, no. 2, pp. 422–438, feb 2019.

[61] MINISTRY OF TRANSPORT AND CIVIL AVIATION, "Civil Aircraft Accident, Report of the Court of Inquiry into the Accidents to Comet G-ALYP on 10th January, 1954 and Comet G-ALYY on 8th April, 1954, url = https://lessonslearned.faa.gov/Comet1/G-ALYP_Report.pdf, year = 1955," Tech. Rep.

[62] Y. Miyano, M. Nakada, M. K. McMurray, and R. Muki, "Prediction of flexural fatigue strength of crfp composites under arbitrary frequency, stress ratio and temperature," *Journal of Composite Materials*, vol. 31, no. 6, pp. 619–638, 1997. [Online]. Available: https://doi.org/10.1177/002199839703100605

[63] F. Mølholt Jensen and K. Branner, "1 - introduction to wind turbine blade design," in *Advances in Wind Turbine Blade Design and Materials*, ser. Woodhead Publishing Series in Energy, P. Brøndsted and R. P. Nijssen, Eds. Woodhead Publishing, 2013, pp. 3 – 28. [Online]. Available: http://www.sciencedirect.com/science/article/pii/B9780857094261500015

[64] J. F. Mougaard, P. N. Poulsen, and L. O. Nielsen, "A partly and fully cracked triangular XFEM element for modeling cohesive fracture," *International Journal for Numerical Methods in Engineering*, vol. 85, no. 13, pp. 1667–1686, apr 2011. [Online]. Available: http://doi.wiley.com/10.1002/nme.3040

[65] B. Natarajan, J. Lee, J. Lim, and S. Shin, "Structural analysis of composite wind turbine blade using advanced beam model approach," *International Journal of Precision Engineering and Manufacturing*, vol. 13, no. 12, pp. 2245–2250, Dec 2012. [Online]. Available: https://doi.org/10.1007/s12541-012-0298-6

[66] National Transportation Safety Board, Bureau of Accident investigation, "Aircraft accident report, Aloha Airlines, flight 243," National Transportation Safety Board, Washington D.C., Tech. Rep., 1989. [Online]. Available: https://www.ntsb.gov/investigations/AccidentReports/Reports/AAR8903.pdf

[67] A. Needleman, "A Continuum Model for Void Nucleation by Inclusion Debonding," *Journal of Applied Mechanics*, vol. 54, no. 3, pp. 525–531, 09 1987. [Online]. Available: https://doi.org/10.1115/1.3173064

[68] H. Neuber, "Theory of Stress Concentration for Shear-Strained Prismatical Bodies With Arbitrary Nonlinear Stress-Strain Law," *Journal of Applied Mechanics*, vol. 28, no. 4, pp. 544–550, 12 1961. [Online]. Available: https://doi.org/10.1115/1.3641780

[69] T. C. Nguyen, Y. Bai, X.-L. Zhao, M. R. Bambach, and R. Al-Mahaidi, "Temperature effect on adhesively bonded cfrp and steel double strap joints," in *Advances in FRP Composites in Civil Engineering*, L. Ye, P. Feng, and Q. Yue, Eds. Berlin, Heidelberg: Springer Berlin Heidelberg, 2011, pp. 877–880.

[70] R. Nicoletti, "Linearization of embedded patterns for optimization of structural natural frequencies," *Journal of the Brazilian Society of Mechanical Sciences and Engineering*, vol. 41, no. 12, p. 545, Nov 2019. [Online]. Available: https://doi.org/10.1007/s40430-019-2040-0

[71] P. Nielsen, P. Berring, C. Pavese, and K. Branner, *Rotor blade full-scale fatigue testing technology and research*, ser. DTU Wind Energy E. Denmark: DTU Wind Energy, 2013, no. 0041.

[72] Nielsen, Per Hørlyk, et. al., "Full scale test ssp 34m blade, combined load. data report," *Danmarks Tekniske Universitet, Risø Nationallaboratoriet for Bæredygtig Energi*, 2011.

[73] P. Noever Castelos and C. Balzani, "The impact of geometric non-linearities on the fatigue analysis of trailing edge bond lines in wind turbine rotor blades," *Journal of Physics: Conference Series*, vol. 749, p. 012009, 09 2016.

[74] M. Nossek and S. Marzi, "Cohesive zone modeling for adhesives," in *Predictive Modeling of Dynamic Processes: A Tribute to Professor Klaus Thoma.* Springer US, 2009,

pp. 89–105. [Online]. Available: https://link-springer-com.zorac.aub.aau.dk/chapter/10.1007/978-1-4419-0727-1{_}5

[75] S. Obata, K. Takahashi, and K. Inaba, "Laminate design for a tapered FRP structure with ply drop-off based on yielding of resin pockets," *Composite Structures*, vol. 253, p. 112787, dec 2020.

[76] M. J. Owen and J. R. Griffiths, "Evaluation of biaxial stress failure surfaces for a glass fabric reinforced polyester resin under static and fatigue loading," *Journal of Materials Science*, vol. 13, no. 7, pp. 1521–1537, jul 1978. [Online]. Available: https://link.springer.com/article/10.1007/BF00553209

[77] N. Perez, *Fracture Mechanics: Second edition*. Springer International Publishing, jan 2017. [Online]. Available: https://www.springer.com/gp/book/9783319249971

[78] Plausinis, "Application of a new constant G load-jig to creep crack growth in adhesive joints," *International Journal of Adhesion and Adhesives*, vol. 15, no. 4, pp. 225–232, 1995.

[79] K. R. Rao, *Wind Energy: Technical Considerations – Contents, Wind Energy for Power Generation: Meeting the Challenge of Practical Implementation*. Cham: Springer International Publishing, 2019, pp. 1–426. [Online]. Available: https://doi.org/10.1007/978-3-319-75134-4_1

[80] J. R. Rice, "A Path Independent Integral and the Approximate Analysis of Strain Concentration by Notches and Cracks," *Journal of Applied Mechanics*, vol. 35, no. 2, pp. 379–386, jun 1968. [Online]. Available: https://asmedigitalcollection.asme.org/appliedmechanics/article/35/2/379/392117/A-Path-Independent-Integral-and-the-Approximate

[81] J. Rice, "Contained plastic deformation near cracks and notches under longitudinal shear," *International Journal of Fracture*, vol. 2, pp. 426–447, 01 1966.

[82] M. Rosemeier, A. Antoniou, and C. Lester, "Sub-components of wind turbine blades: Proof of a novel trailing edge testing concept," in *Mechanics of Composite, Hybrid and Multifunctional Materials, Volume 5*, P. R. Thakre, R. P. Singh, and G. Slipher, Eds. Cham: Springer International Publishing, 2019, pp. 267–274.

[83] H. P. Rossmanith, "George Rankin Irwin-The Father of Fracture Mechanics 1907-1998," *Fragblast*, vol. 2, no. 2, pp. 123–141, jan 1998. [Online]. Available: http://www.tandfonline.com/doi/abs/10.1080/13855149809408882

[84] G. I. Schuëller and H. J. Pradlwarter, "On the stochastic response of nonlinear fe models," *Archive of Applied Mechanics*, vol. 69, no. 9, pp. 765–784, Nov 1999. [Online]. Available: https://doi.org/10.1007/s004190050255

[85] J. Sjølund and E. Lund, "Structural gradient based sizing optimization of wind turbine blades with fixed outer geometry," *Composite Structures*, vol. 203, pp. 725–739, Nov. 2018.

[86] ——, "Composite thickness optimization of offshore wind turbine blade with fixed outer geometry," in *30th Nordic Seminar on Computational Mechanics NSCM30 Proceedings*, ser. Proceedings of the Nordic Seminar on Computational Mechanics, (NSCM). DTU Mechanical Engineering, Oct. 2017, pp. 184–187, 30th Nordic Seminar on Computational Mechanics, NSCM30 ; Conference date: 25-10-2017 Through 27-10-2017.

[87] B. F. Sørensen, S. Goutianos, and T. K. Jacobsen, "Strength scaling of adhesive joints in polymer matrix composites," *International Journal of Solids and Structures*, vol. 46, no. 3, pp. 741 – 761, 2009. [Online]. Available: http://www.sciencedirect.com/science/article/pii/S0020768308003971

[88] B. F. Sørensen, K. Jørgensen, T. K. Jacobsen, and R. C. Østergaard, "DCB-specimen loaded with uneven bending moments," *International Journal of Fracture*, vol. 141, no. 1-2, pp. 163–176, sep 2006. [Online]. Available: https://link.springer.com/article/10.1007{%}2Fs10704-006-0071-x

[89] J. Sørensen and H. Toft, "Probabilistic design of wind turbines," *Energies*, vol. 3, 02 2010.

[90] J. E. Spowart, N. Gupta, and D. Lehmhus, "Additive manufacturing of composites and complex materials," *JOM*, vol. 70, no. 3, pp. 272–274, Mar 2018. [Online]. Available: https://doi.org/10.1007/s11837-018-2742-2

[91] G. H. Staab, "1 - introduction to composite materials," in *Laminar Composites (Second Edition)*, second edition ed., G. H. Staab, Ed. Butterworth-Heinemann, 2015, pp. 1 – 16. [Online]. Available: http://www.sciencedirect.com/science/article/pii/B9780128024003000015

[92] ——, "5 - lamina failure theories," in *Laminar Composites (Second Edition)*, second edition ed., G. H. Staab, Ed. Butterworth-Heinemann, 2015, pp. 139 – 187. [Online]. Available: http://www.sciencedirect.com/science/article/pii/B9780128024003000052

[93] Z. Suo and J. W. Hutchinson, "Interface crack between two elastic layers," *International Journal of Fracture*, vol. 43, pp. 1–18, 1990.

[94] The Guardian. (2009) Speculation grows over mysterious wind turbine damage. https://www.theguardian.com/environment/2009/jan/08/wind-turbine-ufo-lincolnshire-the-sun, last accessed on 19/08/19.

[95] S. Timoshenko and J. Goodier, *Theory of Elasticity*, ser. Engineering societies monographs. McGraw-Hill, 1951. [Online]. Available: https://link.springer.com/chapter/10.1007/1-4020-7861-7_1

[96] A. Turon, B. Bak, E. Lindgaard, C. Sarrado, and E. Lund, "Interface elements for fatigue-driven delaminations in advanced composite materials," *Numerical Modelling of Failure in Advanced Composite Materials*, pp. 73–91, jan 2015. [Online]. Available: https://www.sciencedirect.com/science/article/pii/B9780081003329000037?via{%}3Dihub

[97] V. Tvergaard and J. W. Hutchinson, "The relation between crack growth resistance and fracture process parameters in elastic-plastic solids," *Journal of the mechanics and physics of solids*, vol. 40, no. 6, pp. 1377–1397, 1992.

[98] A. P. Vassilopoulos and T. Keller, "Fatigue of Adhesively-Bonded GFRP Structural Joints." Springer, London, 2011, pp. 141–154. [Online]. Available: http://link.springer.com/10.1007/978-1-84996-181-3{_}5

[99] H. M. Westergaard, "Bearing Pressures and Cracks," *Journal of Applied Mechanics, Vol. 6, pp. A49-53*, 1939.

[100] M. Yangui, S. Bouaziz, M. Taktak, M. Haddar, and A. El-Sabbagh, "Nonlinear analysis of twisted wind turbine blade," *Journal of Mechanics*, vol. 34, no. 3, p. 269â"278, 2018.

[101] G. Yuan and Y. Chen, "Geometrical nonlinearity analysis of wind turbine blade subjected to extreme wind loads," in *Computational Structural Engineering*, Y. Yuan, J. Cui, and H. A. Mang, Eds. Dordrecht: Springer Netherlands, 2009, pp. 521–528.

[102] A. T. Zehnder, "Criteria for elastic fracture," in *Lecture Notes in Applied and Computational Mechanics*. Springer Verlag, 2012, vol. 62, pp. 55–76.

[103] ——, "Determining K and G," in *Lecture Notes in Applied and Computational Mechanics*. Springer Verlag, 2012, vol. 62, pp. 77–107.

[104] ——, "Energy flows in elastic fracture," in *Lecture Notes in Applied and Computational Mechanics*. Springer Verlag, 2012, vol. 62, pp. 33–54.

[105] A. P. Zieliński and F. Frey, "On linearization in non-linear structural finite element analysis," *Computers & Structures*, vol. 79, no. 8, pp. 825–838, Mar 2001. [Online]. Available: http://www.sciencedirect.com/science/article/pii/S0045794900001930

All links in references has been accessible on date of thesis submission

ISSN (online): 2446-1636
ISBN (online): 978-87-7210-936-7 AALBORG UNIVERSITY PRESS